Cell Reports

Article

Constitutive DUSP2 expression enhances lymphoid cell proliferation by activating CDK1 and promotes lymphomagenesis

Graphical abstract

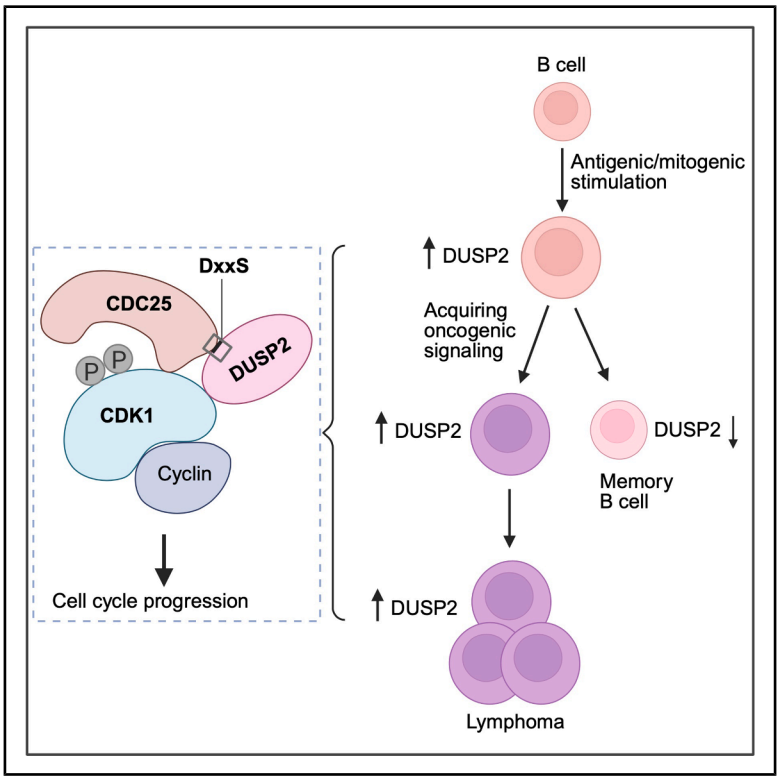

Authors

Yu Qian, Jutatip Panaampon, Bjoern Chapuy, ..., Margaret A. Shipp, Stephanie K. Dougan, Baochun Zhang

Correspondence

baochun_zhang@dfci.harvard.edu

In brief

DUSP2, an immune-restricted dual-specificity phosphatase, is highly expressed in various hematologic malignancies. In B cells, Qian et al. demonstrate that DUSP2 promotes proliferation and malignant transformation through a phosphatase-independent mechanism by engaging CDC25 to activate CDK1 and accelerate cell cycle progression.

Highlights

- *DUSP2* is highly expressed in a wide range of hematologic malignancies
- Constitutive DUSP2 expression promotes B-cell proliferation and lymphomagenesis
- DUSP2 enhances CDK1 activation by recruiting CDC25 via a structural motif
- DUSP2 presents an additional layer of cell cycle regulation in immune cells

Qian et al., 2026, Cell Reports *45*, 117652
July 28, 2026
https://doi.org/10.1016/j.celrep.2026.117652

CellPress

Cell Reports

CellPress
OPEN ACCESS

Article

Constitutive DUSP2 expression enhances lymphoid cell proliferation by activating CDK1 and promotes lymphomagenesis

Yu Qian,[1,2,23] Jutatip Panaampon,[1,2,23] Bjoern Chapuy,[1,2,3,23] Xueyan Zhang,[1,4] Xiujuan Zhao,[1,5] Zhe Wang,[1,2] Pengfei Zhang,[6,7] Tongchai Payungwong,[8] Aretina Zhang,[1] Qiang Ke,[1,9] Jing Zhong,[1,10] Ping Yuan,[1,11] Lei Zhang,[1,12] Min Hong,[1,13] Il-Kyu Choi,[1,2,20] Jiankun Guan,[1,2] Dinis Pedro Calado,[14,15] Scott Rodig,[16,21] Olga Pozdnyakova,[16,22] Klaus Rajewsky,[17] Susana A. Godinho,[18] Siwanon Jirawatnotai,[8] Hao Wu,[6,7] Margaret A. Shipp,[1,2] Stephanie K. Dougan,[19] and Baochun Zhang[1,2,19,24,*]

[1]Department of Medical Oncology, Dana-Farber Cancer Institute, Boston, MA 02215, USA
[2]Department of Medicine, Harvard Medical School, Boston, MA 02115, USA
[3]Charité, University Medical Center Berlin, Campus Benjamin Franklin, 12203 Berlin, Germany
[4]School of Basic Medical Sciences, Guangzhou Medical University, Guangzhou 511436, China
[5]Department of Cell Biology, Tianjin Medical University, Tianjin 300070, China
[6]Department of Biological Chemistry and Molecular Pharmacology, Harvard Medical School, Boston, MA, USA
[7]Program in Cellular and Molecular Medicine, Boston Children's Hospital, Boston, MA 02115, USA
[8]Siriraj Center of Research Excellence (SiCORE) for Precision Medicine and Systems Pharmacology, Department of Pharmacology, Faculty of Medicine, Siriraj Hospital, Mahidol University, Bangkok 10700, Thailand
[9]Department of Diagnosis, School of Medicine, Hangzhou Normal University, Hangzhou, Zhejiang 311121, China
[10]Clinical Medical Research Center, First Affiliated Hospital of University of South China, Hengyang, Hunan 421001, China
[11]Department of Thoracic Surgery, First Affiliated Hospital of Zhengzhou University, Zhengzhou, Henan 450052, China
[12]Department of Cardiology, Shanxi Dayi Hospital, Taiyuan, Shanxi 030032, China
[13]Department of Medical Oncology, First Affiliated Hospital of Kunming Medical University, Kunming, Yunnan 650032, China
[14]Immunity and Cancer Laboratory, The Francis Crick Institute, London, UK
[15]Peter Gorer Department of Immunobiology, Kings College London, London, UK
[16]Department of Pathology, Brigham and Women's Hospital, Boston, MA 02115, USA
[17]Immune Regulation and Cancer, Max Delbrück Center for Molecular Medicine, 13125 Berlin, Germany
[18]Barts Cancer Institute, Queen Mary University of London, London EC1M 6BQ, UK
[19]Department of Cancer Immunology and Virology, Dana-Farber Cancer Institute, Boston, MA, USA
[20]Present address: Department of New Biology and New Biology Research Center (NBRC), Daegu Gyeongbuk Institute of Science and Technology (DGIST), Daegu 42988, Republic of Korea
[21]Present address: Department of Pathology, Beth Israel Deaconess Medical Center, Boston, MA 02115, USA
[22]Present address: Division of Hematopathology, Hospital of University of Pennsylvania, Philadelphia, PA 19104, USA
[23]These authors contributed equally
[24]Lead contact
*Correspondence: baochun_zhang@dfci.harvard.edu
https://doi.org/10.1016/j.celrep.2026.117652

SUMMARY

DUSP2 is known as a nuclear dual-specificity phosphatase, highly restricted to immune cells. Its expression is induced by antigenic and mitogenic stimuli and has been implicated in immune cell differentiation and functions. However, its role in immune cell mitotic proliferation and hematologic malignancies has not been rigorously examined. Here, we show *DUSP2* is highly expressed in human B-cell, T cell, and other hematologic malignancies. Ablating *DUSP2* expression in lymphoma cell lines decreases growth and viability. In mice, transgenic Dusp2 expression promotes B-cell and T cell proliferation, and malignant transformation. Mechanistically, DUSP2 promotes cell cycle progression by activating CDK1 through dephosphorylation at inhibitory Tyr15 and Thr14, which is mediated not by its own phosphatase activity, but instead by a structural motif that recruits CDC25 phosphatases. This work reveals an unexpected oncogenic role for DUSP2 in lymphoid malignancies and the function of a structural motif, which represents an appealing target site for therapeutic intervention.

INTRODUCTION

Dual-specificity phosphatases (DUSPs) are a subset of protein tyrosine phosphatases that can dephosphorylate both tyrosine and serine/threonine residues. In humans, the DUSP family comprises 23 members. All DUSPs contain a common phosphatase domain with a core Cys-X_5-Arg (CX_5R) catalytic motif.[1] A subset of DUSPs contain an N-terminal region comprising two CDC25

homology 2 motifs (CH2A and CH2B)[2] and an intervening cluster of basic amino acids known as the kinase-interactive motif (KIM) that binds mitogen-activated protein kinases (MAP kinases or MAPKs); these DUSPs are generally referred to as typical DUSPs or MAPK phosphatases (MKPs) and are localized in the nucleus, cytoplasm, or both.[1,3] Accruing data show that these typical DUSPs may also dephosphorylate non-MAPK proteins, such as STAT3, histone H3, LCK, and others.[3–6] By acting on various MAPK and non-MAPK targets, DUSP family phosphatases regulate diverse cellular processes.

Among the DUSP family members, DUSP2 (also called phosphatase of activated cells 1 [PAC-1]) is the most highly restricted to immune cells.[4,7,8] Its expression is rapidly induced by antigenic or mitogenic stimulation in various immune cells, such as T cells, B cells, mast cells, and other leukocytes.[7–9] Current understanding of DUSP2's function and mechanism(s) of action is limited, and apparently contradictory findings have been reported. Early *in vitro* work in the Jurkat T cell line showed that DUSP2 can dephosphorylate the MAPK member ERK,[10] and based on this finding, DUSP2 was proposed to negatively control mitogenic signaling and T cell effector functions.[11] Yet, a study in *Dusp2*-knockout mice revealed a positive role for Dusp2 in regulating mast cell growth and viability and macrophage effector functions.[8] That work suggested that Dusp2 dephosphorylates (and deactivates) the MAPK member JNK, with the latter negatively regulating ERK through crosstalk,[12] resulting in positive regulation of ERK activity by Dusp2.[8] More recently, other studies in *Dusp2*-knockout mice indicated roles of Dusp2 in modulating Th17 T cell differentiation via dephosphorylation of STAT3[4] and in regulating T cell effector function in a phosphatase-independent manner.[13] Considering that (1) DUSP2 may exert differential regulation of MAPK family members in different types of cells,[1] and the functional impact of MAPKs themselves is often cell type and context dependent[14,15] and (2) DUSP2 may regulate other substrates beyond MAPKs, much more work remains to be done to understand DUSP2's complex biology in the immune system.

So far, little is known of DUSP2's role in the mitotic processes and malignancies of immune cells. Only a few studies have attempted to elucidate DUSP2's function in cancers, but these were carried out exclusively in non-hematologic cancer cell lines, where DUSP2 appears to play a tumor suppressor role by dephosphorylating ERK.[16,17] This view of a growth-suppressing role apparently conflicts with the long-known high expression of DUSP2 in human T cell leukemia virus (HTLV)-transformed T cells and in various mouse B-cell lymphomas.[7,9,18] Following this lead in studying DUSP2 in B- and T-lineage cells, we reveal an unexpected mechanism by which DUSP2 promotes lymphoid cell proliferation and malignant transformation.

RESULTS

DUSP2 is highly expressed in a wide array of hematologic malignancies

We inspected *DUSP2* expression in a wide range of human cancers by mining publicly accessible data. First, we assessed *DUSP2* transcript levels in a large collection of human cancer cell lines; this analysis revealed a much higher expression in hematologic malignancies of B, T, and myeloid lineages, compared with non-hematologic cancers (Figure 1A). The high expression within several types of B-cell malignancies—mantle cell lymphoma, diffuse large B-cell lymphoma (DLBCL), Burkitt lymphoma, Hodgkin lymphoma, B-cell lymphoblastic leukemia, and others—prompted us to analyze additional B-cell lymphoma/leukemia datasets where normal B cells were available as control. *DUSP2* transcripts were highly elevated in essentially all cases of human B-cell malignancies, compared with normal resting (naive) B cells (Figure 1B).[19–21] We also analyzed *DUSP2* expression in normal B cells at several functional differentiation stages, including germinal center (GC) B cells (centroblasts and centrocytes) and post-GC B cells (memory and plasma cells), in comparison with naive B cells. *DUSP2* expression waxes and wanes along with the GC reaction (Figure 1B), a physiological process whereby B cells mount antigen-specific responses via clonal expansion, affinity maturation, and functional differentiation (see discussion). We compared *DUSP2* expression in activated B cell (ABC)-like DLBCLs versus germinal center B cell (GCB)-like DLBCLs, two major subtypes of DLBCL,[22] but detected no differential expression (data not shown).[23–25] Overall, these analyses show that *DUSP2* is highly expressed in a wide array of human hematologic malignancies, in addition to the previously reported HTLV-associated adult T cell leukemia.[7,18]

The causes of constitutive *DUSP2* expression in the various hematologic malignancies are largely unknown, except in adult T cell leukemia where the HTLV-encoded oncoprotein Tax is known to play a major role.[18] Among B-cell malignancies, DLBCL is the most common lymphoid malignancy in adults and has been characterized in great detail, providing us with opportunities to search for potential mechanism(s) of *DUSP2* high expression in this disease. We queried publicly available data and our recent genomic analysis of 304 primary DLBCLs[25] but found no evidence of *DUSP2* copy number gain in primary DLBCLs or any DLBCL cell lines in the CCLE database (data not shown). *DUSP2* is targeted infrequently by somatic mutations (in 4%–7% human DLBCLs[25–29]), and these mutations lie outside of key functional motifs of the protein and do not cluster at any amino acid position (data not shown). Analysis of the *Dusp2* coding sequence in 12 lymphomas in our mouse model of DLBCL pathogenesis[30] identified also infrequent, sporadic mutations (2 missense and 1 silent; Figures S1A and S1B); and functional assessment of the derived mutants revealed no difference from the wild-type protein (see below).

Because we could not identify a genetic cause within the *DUSP2* locus accounting for the universal *DUSP2* high expression in DLBCL, we speculated that *DUSP2* is transcriptionally upregulated. DLBCL malignancy is fueled by constitutive signaling through B cell receptor (BCR) and/or NF-κB pathways.[31] Activation of these pathways in primary B cells using anti-IgM for BCR activation, or anti-CD40 or LPS treatment for NF-κB activation induced *Dusp2* expression (Figure S2); and inhibition of these pathways (by chemical and genetic means) in human DLBCLs is known to result in decreased *DUSP2* expression[32,33] Thus, it is likely that the constitutive *DUSP2* high expression in DLBCLs is at least partly due to chronic BCR and/or NF-κB signaling.

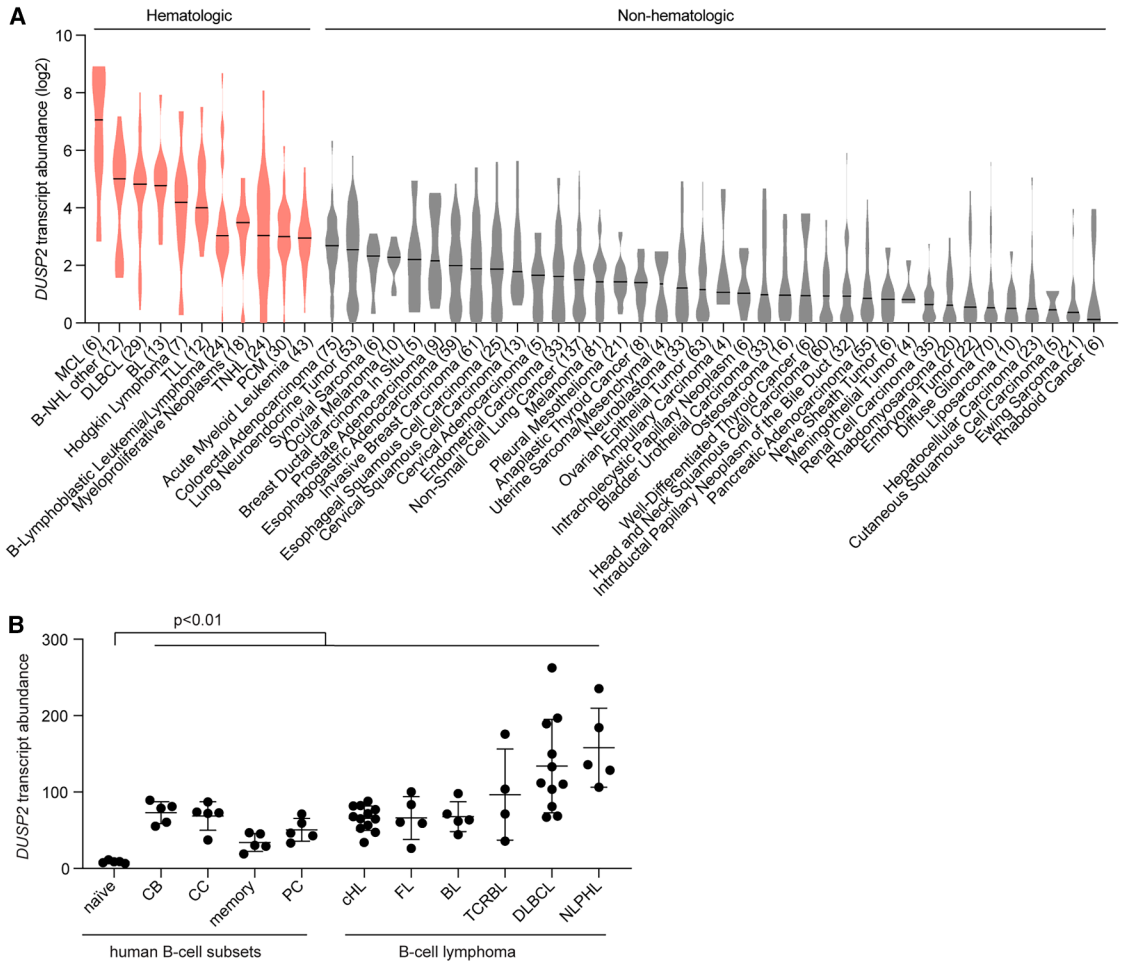

Figure 1. *DUSP2* is highly expressed in various hematologic malignancies

(A) *DUSP2* expression profiles in various types of cancers from the Cancer Cell Line Encyclopedia (CCLE) database. MCL, mantle cell lymphoma; B-NHL, B-cell non-Hodgkin lymphoma; DLBCL, diffuse large B-cell lymphoma; BL, Burkitt lymphoma; TLL, T-lymphoblastic leukemia/lymphoma; TNHL, T cell non-Hodgkin lymphoma; PCM, plasma cell myeloma. Number of cell lines per tumor type is shown in parentheses.

(B) *DUSP2* expression in a representative panel of different human B-cell lymphomas (right) and normal B cells at the indicated differentiation stages (left). Data were derived from the GSE12453 dataset. cHL, classical Hodgkin lymphoma; NLPHL, nodular lymphocyte-predominant HL; TCRBL, T cell rich B-cell lymphoma; FL, follicular lymphoma; CB, centroblasts; CC, centrocytes; PC, plasma cells. *p* value by two-sided Mann-Whitney U test.

Lymphoma cell addiction to DUSP2 expression

The constitutively high expression of *DUSP2* in various hematologic malignancies and the absence of genetic alterations in the *DUSP2* locus in most human DLBCLs appear incompatible with previous studies in non-hematologic cell lines, which suggested that DUSP2 plays a tumor-suppressing role.[16,17] We therefore decided to investigate the function of DUSP2 in hematologic malignancies, with a focus on the B-cell lineage.

We used CRISPR to generate deletion or insertion mutations of *Dusp2* in a mouse (GCB type) DLBCL cell line 775 that was derived from a *Bcl6* transgenic mouse[30] and expresses wild-type *Dusp2* alleles. A single guide RNA targeting *Dusp2* coding exon 1 created mostly frameshift mutations. However, when the cells were transplanted into immunodeficient hosts, the cells that grew out carried only deletions of three nucleotides (in-frame), which likely caused minimal changes to the protein sequence. This suggested that the majority of cells with frameshift mutations that caused loss of protein expression were negatively selected (Figures 2A and 2B). Furthermore, shRNA-mediated knockdown of *DUSP2* in representative human DLBCL cell lines (DHL4, GCB type; HBL1 and TMD8, both ABC type) resulted in marked cell apoptosis (Figures 2C and S3A). We also noted that knockdown of *DUSP2* led to decreased cell proliferation, as indicated by delayed CellTrace dilution (Figure 2D). Together, these data indicate that DUSP2 expression is crucial for lymphoma cell growth and viability *in vitro* and *in vivo*.

Ectopic expression of Dusp2 enhances lymphoma and primary lymphocyte proliferation

We ectopically expressed wild-type (WT) Dusp2 in the mouse DLBCL cell line 775 and found that it notably enhanced

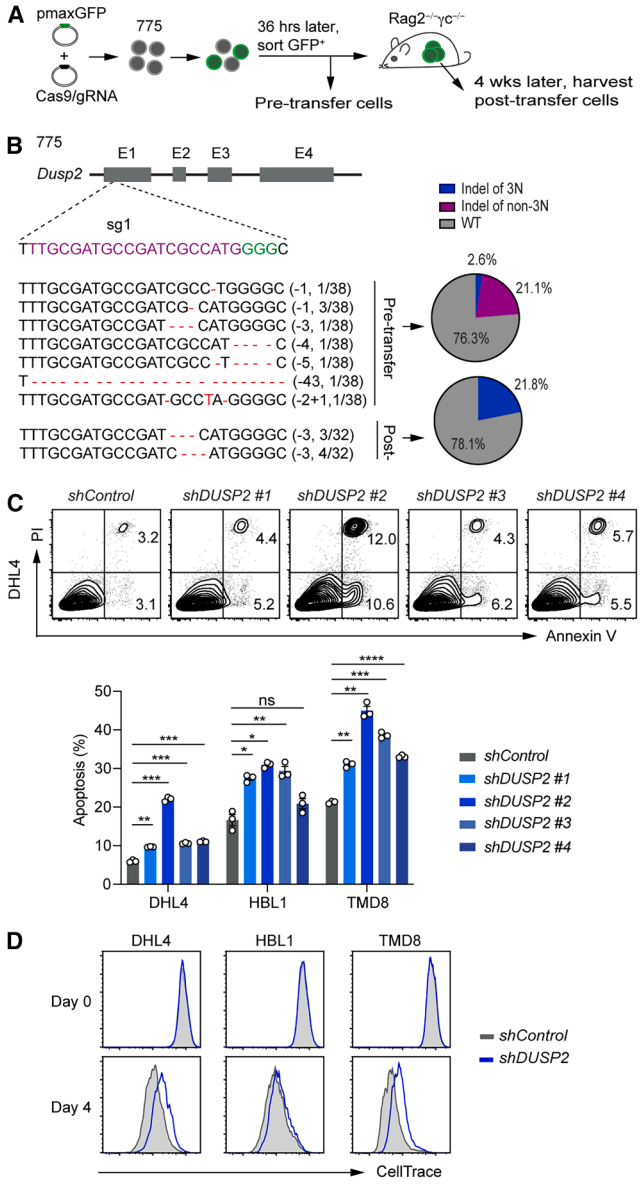

Figure 2. DUSP2 expression is crucial for lymphoma cell growth and viability

(A and B) Mouse DLBCL 775 cells treated by CRISPR-Cas9/gRNA (sg1), pre- or post-transfer in immunodeficient mice, per the scheme in (A) were sequenced for the targeted *Dusp2* exon region and the rates of indel mutations of 3N and non-3N in pre- or post-transfer cells were calculated and shown (B). Data are pooled from two independent experiments.

(C and D) Human DLBCL cell lines were transduced with shRNAs against *DUSP2* or vector control, and immediately after the 2-day drug selection were assayed for apoptosis by Annexin V/PI staining (C, showing FACS plots and summary data) and proliferation by CellTrace dilution (D, showing FACS plots; gated on viable cells). Data are representative of two independent experiments. Error bars denote mean ± SD of 3 replicate assays in a representative experiment. ns, not significant; $*p < 0.05$, $**p < 0.01$, $***p < 0.001$, $****p < 0.0001$, unpaired two-tailed Student's *t* test.

lymphoma cell viability and proliferation *in vitro* (Figures 3A, 3B, and S3B); it also significantly promoted tumor growth upon transfer of the cells into immunodeficient hosts, compared with the vector control (Figures 3C and 3D). Our parallel testing (in the 775 cells) of the mouse lymphoma-derived mutants $Dusp2^{G65V}$ and $Dusp2^{V206L}$ (see Figure S1) in the above assays revealed no functional difference from WT Dusp2 (data not shown), suggesting that these Dusp2 mutations represent passenger mutations. As in the mouse system, ectopic expression of WT DUSP2 in human DLBCL cells led to enhanced proliferation (Figures 3E and S3C).

These results in mouse and human DLBCL cell lines demonstrate that DUSP2 has growth-promoting function and suggest that DUSP2 overexpression might promote B-cell transformation. To test this hypothesis, we generated a Rosa26 knock-in allele allowing expression of WT Dusp2 with a GFP reporter through excision of a transcriptional/translational Stop cassette via Cre/LoxP-mediated recombination ($Dusp2^{stopFl}$; Figure 3F). To assess whether enforced Dusp2 expression in primary B cells has pro-proliferative function, as it does in transformed B cells, we crossed $Dusp2^{stopFl}$ mice and control YFP^{stopFl} mice[34] to *CD19-cre* mice,[35] and then harvested reporter$^+$ B cells for *ex vivo* and *in vitro* analyses. Although enforced Dusp2 expression in primary B cells was not sufficient to trigger their proliferation, it markedly enhanced their proliferation upon mitogenic stimulation with anti-CD40 plus IL-4 or LPS (Figure 3G). Of note, the pro-proliferative effect of Dusp2 is not restricted to the B-cell lineage, as it was also observed in primary T cells upon mitogenic/antigenic stimulation with anti-CD3 plus anti-CD28 (Figure 3H; in this assay primary T cells were isolated from $Dusp2^{stopFl}$ or YFP^{stopFl} control mice and treated with TAT-Cre to turn on conditional alleles *in vitro*).

Constitutive Dusp2 expression promotes lymphomagenesis

We next sought to assess whether enforced Dusp2 expression in B cells causes lymphomagenesis. Given that most B-cell lymphomas, including DLBCL, arise from transformation of GC B cells, we targeted Dusp2 expression to GC B cells by crossing $Dusp2^{stopFl}$ mice (and control YFP^{stopFl} mice) to *Cγ1-cre* mice[36]; the *Cγ1-cre* transgene allows conditional alleles to be turned on/off in GC B cells by immunizing the mice with sheep red blood cells (SRBCs).[30,37] Assessing *Dusp2* mRNA revealed a significant increase in GC B cells and a remarkable increase in post-GC memory B cells in mice carrying the *Dusp2* knock-in allele compared with control mice (Figure S3D). Considering the possibility that enforced Dusp2 expression alone may not suffice to induce lymphomagenesis, we also tested whether Dusp2 cooperates with a well-characterized *Bcl6* transgene (*IμBcl6*; modeling the *Bcl6* translocation, a major genetic event implicated in ~30% of human DLBCLs[38,39]) in lymphomagenesis. The *Bcl6* transgene was also chosen based on our finding (Figures 3A–3D) that ectopic Dusp2 expression enhances the growth and malignancy of the cell line 775, a *Bcl6* transgene-driven mouse DLBCL line established in our previous work.[30]

The experimental and control mice were immunized with SRBCs twice, at the ages of 2 and 3 months, and monitored for lymphoma development. Sampling two mice each of the $Cγ1\text{-}cre;IμBcl6;Dusp2^{stopFl}$ and $Cγ1\text{-}cre;IμBcl6$ cohorts approximately 2 months after the last immunization revealed that the two $Cγ1\text{-}cre;IμBcl6;Dusp2^{stopFl}$ mice had markedly enlarged spleens

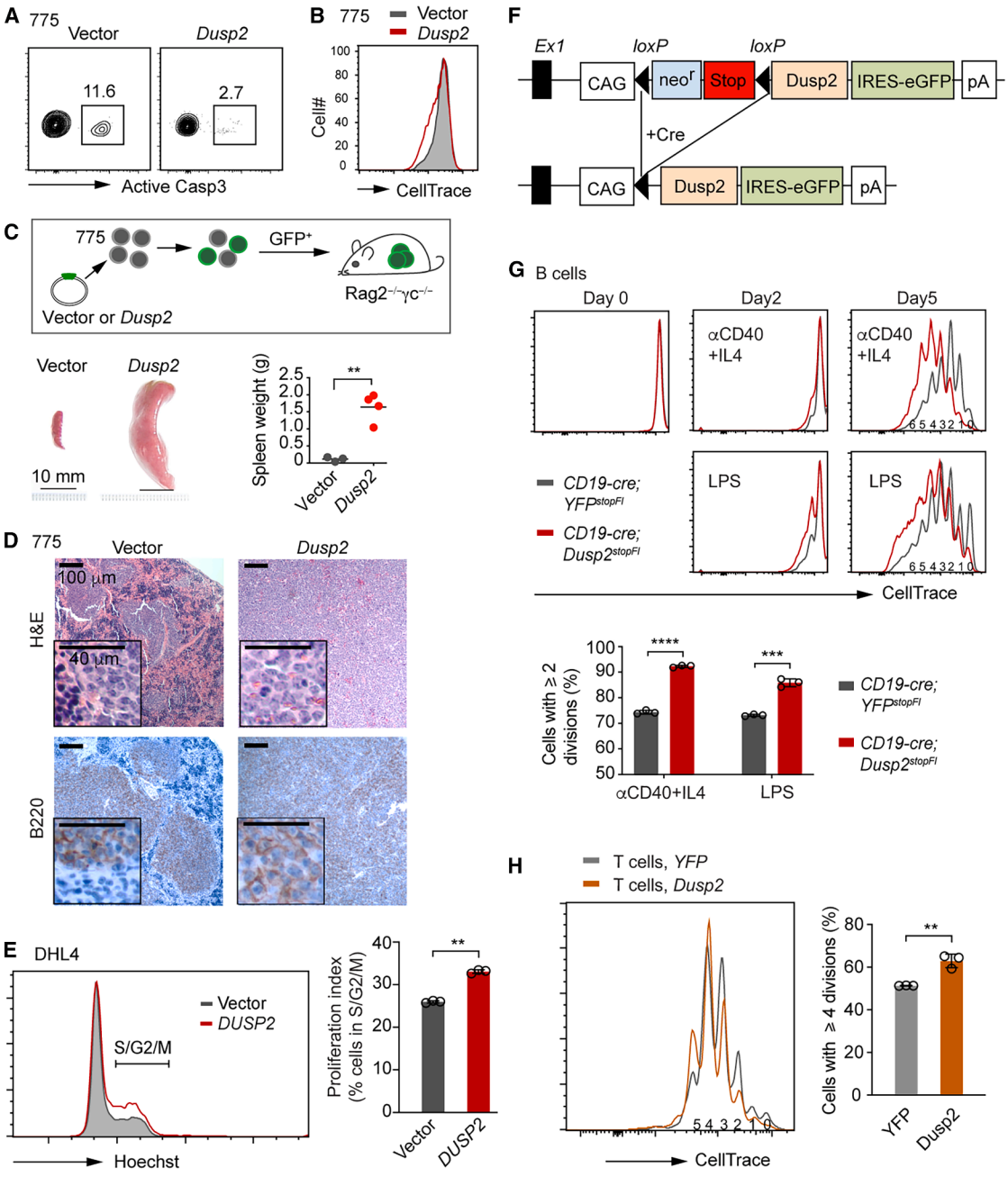

Figure 3. Ectopic expression of Dusp2 promotes lymphoma and primary lymphocyte proliferation

(A and B) The 775 cells were transduced with MSCV encoding *Dusp2* or vector control (all carry an IRES-GFP reporter), and 2 days later assayed for apoptosis by active caspase-3 staining (A) and proliferation by CellTrace dilution (B). GFP$^+$ cells were gated for the analyses.

(C and D) The 775 cells were transduced as in (A), GFP$^+$ cells were FACS sorted and transferred into immunodeficient mice (as depicted in C, top). 24 days later, recipients were euthanized and tumor growth in the spleen was assessed by spleen size and weight (C, bottom), histological and immunohistochemical analyses (D). Scale bars, 100 μm; inset scale bars, 40 μm.

(E) Human DLBCL DHL4 cells were transduced to express DUSP2 or vector control, stained with Hoechst 33342 and analyzed by FACS. FACS plots and the calculated proliferation indexes are shown.

(F) Schematic representation of the strategy for targeting the conditional *Dusp2*^{stopFl} allele into Rosa26 locus.

(G) Splenic B cells were isolated from *CD19-cre;YFP*^{stopFl} or *CD19-cre;Dusp2*^{stopFl} mice, treated with the indicated stimuli and assayed for proliferation by CellTrace dilution. FACS plots and the calculated percentages of cells with ≥2 divisions at day 5 are shown.

(legend continued on next page)

with a DLBCL-like disease, characterized by a diffuse growth pattern of large cells, while the two *Cγ1-cre;IμBcl6* mice exhibited only slightly enlarged spleens with mild follicular hyperplasia, compared with age-matched normal C57BL/6 mice (Figures S4A and S4B). PCR analysis of IgH gene rearrangements detected a clonal B cell population in the spleen of each of the *Cγ1-cre;IμBcl6;Dusp2*^{stopFl} mice, but not the two *Cγ1-cre;IμBcl6* mice (Figure S4C). These data suggest that enforced Dusp2 expression may promote lymphomagenesis, at least when combined with the *Bcl6* transgene. Indeed, this was confirmed by analysis of larger numbers of mice monitored up to the age of 80 weeks (18 months). Within the observation period, *Cγ1-cre;IμBcl6;Dusp2*^{stopFl} mice displayed significantly earlier onset and higher incidence of fatal lymphomas than *Cγ1-cre;IμBcl6* mice (81% vs. 41%). Only a low fraction (2/26) of *Cγ1-cre;Dusp2*^{stopFl} mice succumbed, at late ages (around 18 months), to DLBCL-like disease (Figure 4A; Table S1); none of the control *Cγ1-cre;YFP*^{stopFl} mice succumbed to any disease (Figure 4A).

The lymphomas in both *Cγ1-cre;IμBcl6;Dusp2*^{stopFl} and *Cγ1-cre;IμBcl6* groups involved the spleen and lymph nodes (sometimes non-lymphoid organs as well), and most of the cases exhibited a DLBCL-like disease (Figures 4A–4C; Table S1).[30] Analysis of IgH gene rearrangements revealed the lymphomas were of clonal B cell origin (Figure 4D). Immunohistochemical analysis showed that the lymphomas in *Cγ1-cre;IμBcl6;Dusp2*^{stopFl} mice were B220^{+}GFP^{+}, confirming their expression of the knock-in *Dusp2* allele (Figure 4E). Furthermore, sequence analysis of the rearranged IgH V regions from clonal B cell tumors revealed somatically mutated Ig genes in four of the five *Cγ1-cre;IμBcl6;Dusp2*^{stopFl} tumors and two of the three *Cγ1-cre;IμBcl6* tumors (Table S2), suggesting that most of the tumors derived from GC or post-GC B cells. The rearranged IgH V region was successfully cloned from one of the two *Cγ1-cre;Dusp2*^{stopFl} tumors, and sequence analysis revealed a high frequency of mutation (Table S2), suggesting a GC or post-GC B cell origin of the tumor.

Collectively, these data indicate that although enforced *Dusp2* expression alone induces a low rate of B-cell transformation, it significantly accelerates lymphomagenesis in cooperation with deregulated Bcl6. Thus, Dusp2 overexpression plays an oncogenic role in B-cell lymphomagenesis.

DUSP2 activates the cell cycle regulator CDK1 through dephosphorylation of Tyr15 and Thr14

The finding of an oncogenic role for DUSP2 in B-cell malignancy prompted search for the underlying molecular mechanism. MAPK family members—ERK, p38, and JNK—are the most studied DUSP2 substrates, and the literature shows that DUSP2 exerts differential regulation of individual MAPK members in different types of cells.[8,10,40] Likewise, we found that ectopic DUSP2 expression led to pronounced dephosphorylation of ERK and p38 in 293T cells (human embryonic kidney cells), but barely any change in these substrates in DHL4 and HBL1 cells (human DLBCL cells); the latter cells also showed little, if any, dephosphorylation of JNK upon ectopic DUSP2 expression (Figure S5A). Of note, the basal phosphorylation of MAPK members varies dramatically, from undetectable to high levels, in different DLBCL cell lines (Figure S5A).[41] In mouse primary B cells, enforced Dusp2 expression had only a transient effect on ERK phosphorylation at the early phase of B cell activation (Figure S5B). Collectively, these data suggest that the oncogenic function of DUSP2 in B cells may not be executed through regulation of MAPKs.

Further experimentation using DUSP2 site-specific mutants showed that abolishing DUSP2's ability to regulate MAPKs does not affect its pro-growth/viability function in DLBCL cells. Ectopic DUSP2 expression can substantially rescue DLBCL cells from death caused by inhibition of key BCR signaling components[32] (Figure 5A); this finding, together with other data suggesting DUSP2 is a transcriptional target of BCR signaling (see above), implies that the pro-growth/viability function of chronic BCR signaling is partly relayed by DUSP2. In these same cells, ectopic expression of a DUSP2 mutant ΔKIM that abolishes interaction with MAPKs (ERK, p38, and JNK), or the C257S substitution that abrogates phosphatase activity to MAPKs (as well as STAT3),[4,8] both rescued DLBCL cells from BCR inhibition to similar extents as WT DUSP2 (Figure 5B; see validation of the mutants in Figure S5C). These results indicate that DUSP2's pro-growth/viability function is mediated through as-yet-unknown target(s).

We used immunoprecipitation (IP) followed by mass spectrometry to identify DUSP2-associated proteins in DLBCL cells. Among the identified proteins, CDK1 (also known as CDC2; Figure 5C; Table S3) drew our particular attention because (i) it is the key initiator of mammalian cell mitosis and can also drive all other cell cycle phases, in complex with partner cyclins[42–44]; (ii) its function is known to be activated by dephosphorylation at two inhibitory sites—Tyr15 and Thr14—by CDC25 dual-specificity phosphatases[45]; (iii) DUSP2 has a CDC25 homology domain (see Figure S1B). Thus, if DUSP2 acted like CDC25 to activate CDK1, that could explain its pro-proliferative effect.[46] We confirmed the physical association between DUSP2 (with a FLAG tag) and CDK1 in co-IP assays with an anti-CDK1 antibody (Figures 5D and 5E).

We then tested whether DUSP2 regulates CDK1 activity by dephosphorylating Tyr15 and Thr14. Indeed, ectopic expression of DUSP2 in DLBCL cells resulted in reduced phosphorylation of Tyr15 (pY15) and Thr14 (pT14) on CDK1 (Figure 5F). Conversely, shRNA-mediated knockdown of DUSP2 led to markedly increased phosphorylation at these sites (Figure 5G). Therefore, the pro-proliferative effect of DUSP2 (see

(H) Splenic CD4^{+} T cells were isolated from *YFP*^{stopFl} or *Dusp2*^{stopFl} mice, treated with TAT-Cre *in vitro*, followed by anti-CD3 plus anti-CD28 stimulation for 3 days, and then assayed for proliferation by CellTrace dilution. Analyses were gated on YFP/GFP reporter-positive cells. FACS plots and the calculated percentages of cells with ≥4 divisions are shown.

Data in (A)–(E) and (G)–(H) are representative of two independent experiments. Bars in (C) denote mean of biological replicates in each group in a representative experiment; in (E), (G), and (H) denote mean ± SD of 3 replicate assays in a representative experiment. $^{**}p < 0.01$, $^{***}p < 0.001$, $^{****}p < 0.0001$, unpaired two-tailed Student's *t* test.

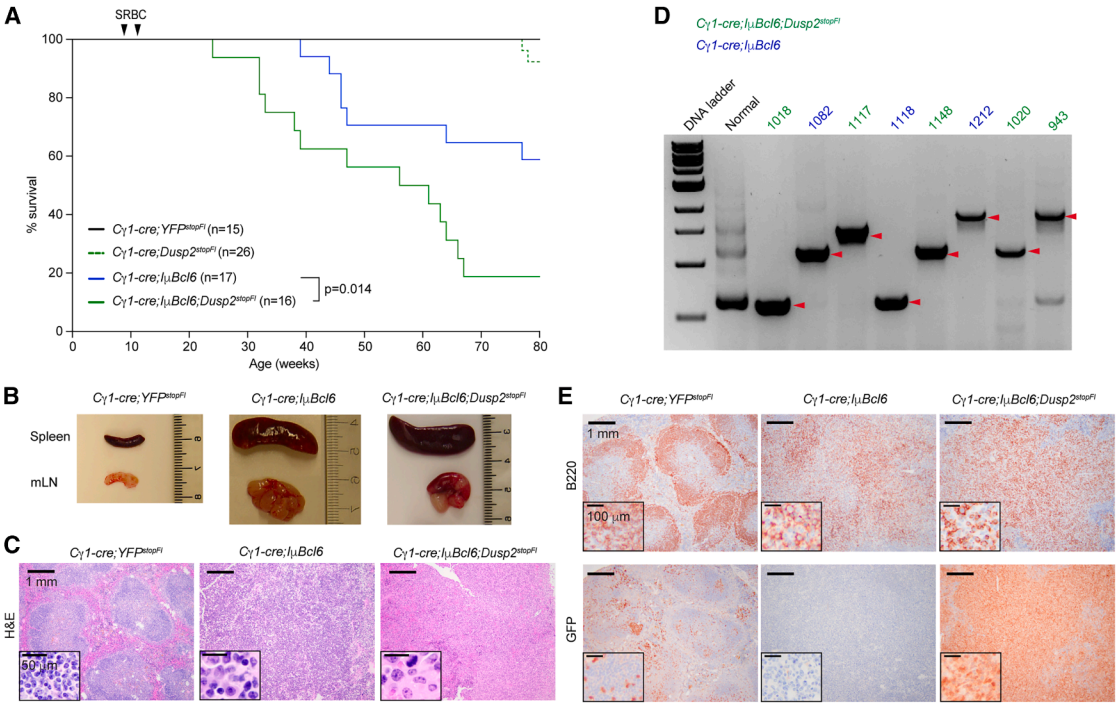

Figure 4. Enforced expression of Dusp2 cooperates with Bcl6 in B-cell lymphomagenesis

(A) Kaplan-Meier survival curves of mice of the indicated genotypes. *p* value by log rank test.

(B and C) Representative pictures of the spleen and mesenteric lymph nodes (mLN) (B) and H&E staining of spleen sections (C) from control *Cγ1-cre;YFP*^{stopFl}, and tumor-bearing *Cγ1-cre;IμBcl6* and *Cγ1-cre;IμBcl6;Dusp2*^{stopFl} mice. Scale bar, 1 mm; inset scale bar, 50 μm.

(D) PCR analysis of rearranged IgH VDJs in representative biopsies from the indicated mice, as compared to a normal spleen. A polyclonal B cell population is denoted by the presence of four major bands, corresponding to rearrangements utilizing the four JH segments; a monoclonal population is reflected by the amplification of a single or predominant band (red arrowhead).

(E) Representative immunohistochemical staining of B220 (upper) and GFP (lower) on spleen sections from control *Cγ1-cre;YFP*^{stopFl}, and tumor-bearing *Cγ1-cre;IμBcl6* and *Cγ1-cre;IμBcl6;Dusp2*^{stopFl} mice. Scale bars, 1 mm; inset scale bars, 100 μm.

Data in (B), (C), and (E) are representative of analyses done in 4–6 mice of each genotype.

Figures 3B–3E, 3G, and 3H) could be explained by its ability to enhance CDK1 activation through dephosphorylation of Tyr15 and Thr14.[46] DUSP2 knockdown, on the other hand, led to reduced cell proliferation, as indicated by an S-phase reduction and G1 cell accumulation (suggesting a partial G1/S arrest; Figure 5H), as well as an M-phase reduction (Figure 5I) and increased ratio of cells in G2/M vs. S phase (Figure 5H) that suggest a partial G2/M arrest. The finding that elevated pY15/pT14 CDK1 (inactive state) correlates with G1/S and G2/M arrest (Figures 5G–5I) is in line with the view that CDK1 not only is essential for G2/M transition but also has a role in G1/S transition.[42–44,47] Furthermore, mitotic failure may culminate in cellular demise as seen in Figure 2C.[48] In keeping with our earlier finding that the pro-growth/viability function of DUSP2 in DLBCL cells is not mediated through the KIM motif and the catalytic site C257 (Figure 5B), we found that DUSP2's ability to bind and regulate CDK1 is preserved when these motifs are functionally abrogated, as exemplified in the 293T experimental system (Figures 5J and 5K). Taken together, these data suggest that DUSP2 promotes proliferation/viability by activating CDK1 through dephosphorylation of Tyr15 and Thr14, in a manner independent of its classical phosphatase activity.

DUSP2 regulates CDK1 through a novel N-terminal DxxS motif, which recruits CDC25 phosphatases

In seeking to further understand how DUSP2 regulates CDK1 dephosphorylation at Tyr15 and Thr14, we considered two possibilities: either DUSP2 directly catalyzes the dephosphorylation via a cryptic phosphatase motif (distinct from the classical CX_5R motif) or DUSP2 acts indirectly by recruiting/enhancing CDC25s (CDC25A/B/C), the only known phosphatases specialized in dephosphorylating Tyr15 and Thr14 of CDK1.

DUSP2 possesses a CDC25 homology region in its N-terminal half (see Figure S1B and below). This prompted us to search that region for any conserved sequence motif with catalytic potential. While the vast majority of protein tyrosine phosphatases (PTPs) utilize a cysteine as the enzymatic nucleophile, a subgroup of PTPs use an aspartate as the nucleophile and require divalent cations.[49] Interestingly, a previous sequence alignment analysis comparing CDC25 and DUSP2 (PAC-1) pinpointed two conserved Asp-containing motifs in the latter[50] (Figure 6A). To test the possible involvement of the two DUSP2 candidate motifs—DxR_{31-33} and $DxxS_{92-95}$—in CDK1 dephosphorylation, we constructed DUSP2 variants by mutating the most conserved residues of these motifs. Both the D31N/R33A and D92N/S95A

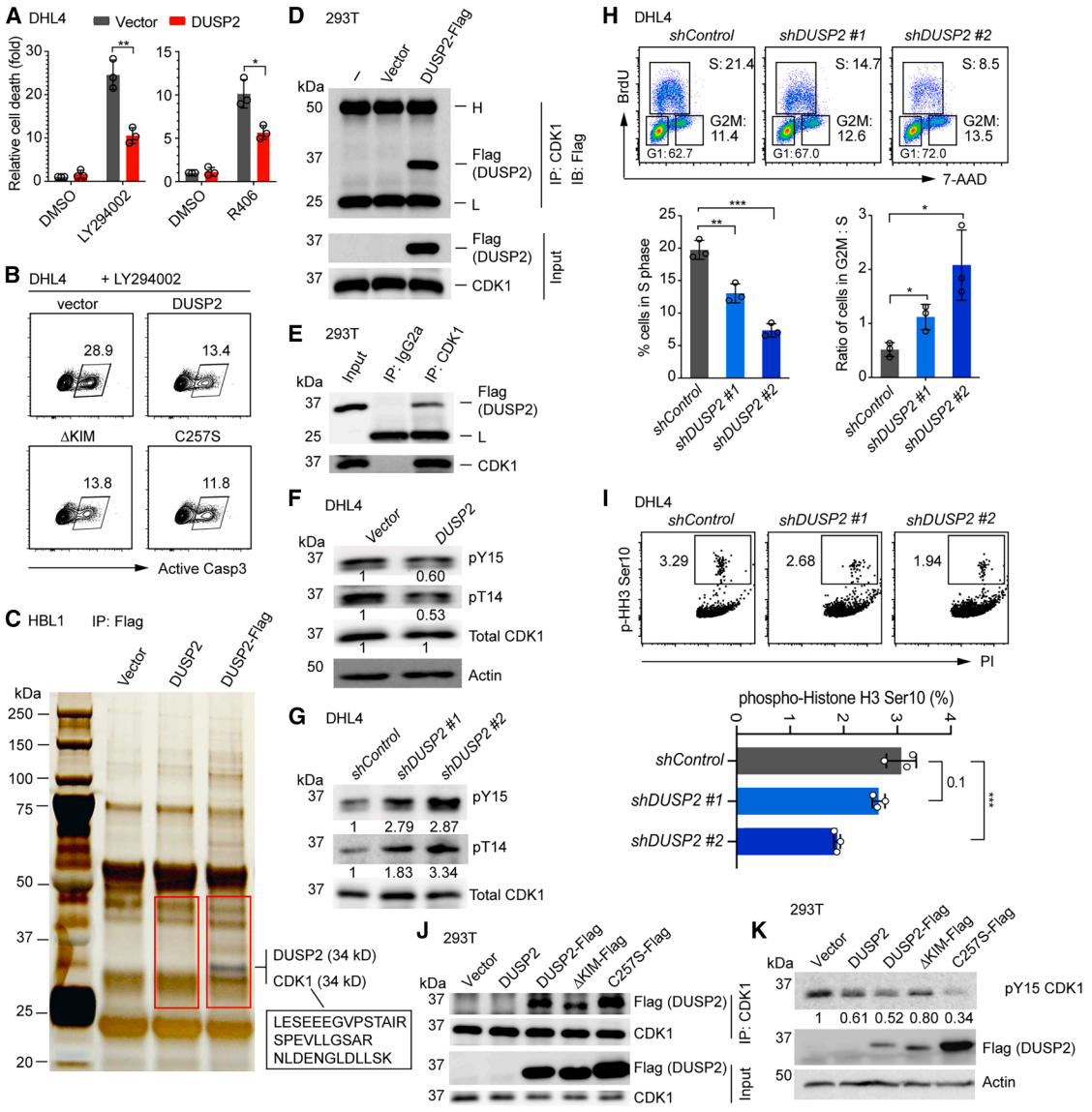

Figure 5. DUSP2 activates CDK1 through dephosphorylation of Tyr15 and Thr14, in a manner independent of its currently known functional motifs

(A) DHL4 cells were transduced with a lentiviral vector encoding DUSP2 or vector control, treated with DMSO (vehicle control) or PI3K inhibitor LY294002 or SYK inhibitor R406 for 2 days, and then assayed for apoptosis by active caspase-3 staining. Cell death in various groups relative to that in DMSO-treated vector control group is shown.

(B) DHL4 cells were transduced with lentiviral vectors encoding DUSP2, DUSP2$^{\Delta KIM}$, DUSP2^{C257S}, or vector control, treated with the PI3K inhibitor LY294002 for 2 days, and then assayed for apoptosis by active caspase-3 staining by FACS. Here, WT and all variants of DUSP2 carry a C-terminal FLAG tag; parallel experiments with non-tagged WT DUSP2 show nearly identical results to Flag-tagged WT DUSP2 and thus are not shown.

(C) Lysates of human DLBCL cells transduced to express DUSP2 with or without FLAG tag were immunoprecipitated with anti-Flag beads, resolved by SDS-PAGE, followed by silver staining; red rectangle-marked areas were excised for mass spectrometry analysis. Right (outlined text), three identified peptide sequences mapping to CDK1.

(D) 293T cells were transfected to express DUSP2-Flag, vector control, or left untransfected, and cell lysates were subjected to immunoprecipitation (IP) with anti-CDK1, followed by immunoblotting (IB) with anti-Flag. H, antibody heavy chain; L, light chain.

(E) 293T cells expressing DUSP2-Flag were subjected to IP with anti-CDK1 or isotype control IgG2a, followed by IB with anti-Flag.

(F) Human DLBCL cells were transduced to express DUSP2 or vector control and subjected to IB analysis with antibodies detecting phospho-Y15 (pY15), phospho-T14 (pT14), or total CDK1, or actin as loading control. Numbers below bands indicate quantifications (normalized to the respective loading controls) relative to the control sample.

(G) Human DLBCL cells were transduced with shRNAs against *DUSP2* or control shRNA, and subjected to IB analysis with antibodies as in (F).

(legend continued on next page)

variants retained the ability to regulate MAPK ERK and JNK (Figure S6A), excluding detrimental structural changes due to these site-specific mutations. We found that, in 293T cells, ectopic expression of the D31N/R33A variant, like the WT DUSP2, resulted in enhanced dephosphorylation of CDK1, while the D92N/S95A variant appeared to lose such function (Figure S6B).

Further quantitative analysis in DLBCL cells established the essential role of the DxxS motif for DUSP2 regulation of CDK1 dephosphorylation. To enable a quantitative measurement of CDK1 Tyr15 phosphorylation in single cells, we employed an intracellular flow cytometry assay using a pY15 CDK1 antibody. The antibody specificity was demonstrated by abrogation of binding by a blocking peptide. We found that, in contrast to WT DUSP2 and other variants, the D92N/S95A variant completely lost the ability to dephosphorylate CDK1 when it was ectopically expressed in DLBCL cells (Figures 6B, 6C, and S6C).

Having identified the essential role of the DxxS motif in regulating CDK1 dephosphorylation, we sought to test whether this was through direct phosphatase activity. We produced high-purity bacterial recombinant proteins consisting of the DUSP2 N-terminal half (aa 2–157, containing the DxxS motif), the full-length protein with a C257S mutation (abolishing the Cys257-associated phosphatase activity), or the C-terminal half (aa 158–314, containing the classical phosphatase motif CX_5R) as a control. Using the standard phosphatase substrate pNPP (in the presence of varying divalent cations; see STAR Methods), we could not detect any *in vitro* phosphatase activity from the recombinant N-terminal half or the C257-mutated full-length protein, while the C-terminal half, as expected, had readily detectable activity (data not shown). Although the possibility of an inactive tertiary structure of the bacterially produced protein cannot be formally excluded, our failure to detect any phosphatase activity in DUSP2's N-terminal half is in line with the general notion that this region is catalytically inactive.

We then tested whether DUSP2 regulates CDK1 dephosphorylation by recruiting/enhancing CDC25s. If so, we reasoned that DUSP2's DxxS motif might mediate the interaction with CDC25s or CDK1. Indeed, by co-IP assays, we demonstrated physical interaction of DUSP2 with both CDK1 and CDC25s (such as CDC25B or CDC25C). The interaction with CDC25s, but not with CDK1, strictly required the DxxS motif (Figure 6D). Both interactions appeared weak, in line with the transient nature of the interaction of phosphatases (and complexes) with their protein substrates.[45] In line with the finding in Figure 6D, confocal imaging analysis in HeLa cells transfected with wild-type DUSP2 versus the D92N/S95A mutant detected significantly more co-localization signals of CDC25C with wild-type DUSP2 than with the mutant (Figure 6E). Furthermore, using the recombinant full-length DUSP2 protein (with the C257S mutation that is irrelevant in DUSP2 regulation of CDK1) in an *in vitro* binding assay, we found that DUSP2 facilitated CDC25 binding to cyclin-CDK1 (Figure 6F). Accordingly, in an *in vitro* phosphatase assay DUSP2 was found to enhance CDC25-mediated dephosphorylation of pY15-CDK1 (Figure 6G).

Taken together, these findings indicate that DUSP2 promotes CDK1 activation by acting as an adaptor to enhance/stabilize the interaction of CDK1 with CDC25s. There is a possibility that such interaction causes conformational changes to increase the phosphatase activity of CDC25s on CDK1. Furthermore, our results identify the DUSP2's N-terminal DxxS motif as its interaction site with CDC25s.

DISCUSSION

We show that *DUSP2* is highly expressed in a wide range of hematologic malignancies. Modeling DUSP2 overexpression *in vivo* in mouse B cells reveals that it promotes proliferation and malignant transformation. DUSP2 exerts its pro-proliferative effect via activation of CDK1 by removing the inhibitory Tyr15 and Thr14 phosphorylation, which is mediated not by its own phosphatase activity, but instead by an N-terminal DxxS motif that recruits CDC25s, the phosphatases specialized in such function.[49] Our results further demonstrate that DUSP2 overexpression similarly potentiates T cell proliferation, suggesting a general role for DUSP2 in immune cell proliferative expansion, as well as transformation.

The establishment of an oncogenic role for DUSP2 in B-cell malignancies stands in contrast to the previously suggested tumor-suppressing role in non-hematologic cancers. The latter notion was proposed on the basis of DUSP2 negatively regulating MAPKs. Perhaps, DUSP2 regulation of MAPKs has a more prominent role in non-hematologic cancers than in B-cell malignancies. In the present work, we find a pronounced function of DUSP2 is to regulate cell cycle progression via activating CDK1. It is noteworthy that the role of DUSP2 overexpression in the transformation of B cells is likely more complex than that of a simple driver of cell proliferation: because of enhanced activity, CDK1 (in complex with partner cyclins) pushes cells to bypass the mitotic checkpoint and potentially other checkpoints, which might result in increased mutation rate and genomic instability.[42] Additionally, DUSP2 may regulate other cellular processes through as-yet-uncharacterized targets (Table S3). By these mechanisms, DUSP2 cooperates with other genetic and epigenetic events,[51–53] such as *BCL6* translocation exemplified in the mouse model, to drive B-cell transformation.

The mechanisms underlying *DUSP2* high expression in hematologic cancers remain largely undefined. It appears that the overexpression of DUSP2, much like that of CDC25s in cancers,[46,54] is fueled by various transformation-associated transcription factors of cellular or viral origin. In DLBCL, this is due,

(H and I) Human DLBCL cells were transduced with shRNAs as in (G) and subjected to cell cycle analysis by BrdU incorporation and 7-AAD staining (H), or phospho-histone H3 (p-HH3) Ser10 staining (a specific marker for mitotic cells; I). In (H), FACS plots and the calculated percentages of cells in S phase and the ratios of cells in G2/M:S phase are shown; in (I), FACS plots and summary data are shown.

(J and K) 293T cells were transfected to express the indicated DUSP2 variants and subjected to IP with anti-CDK1, followed by IB with anti-Flag and anti-CDK1 (J), or directly subjected to IB analysis with the indicated antibodies (K).

Data in (A), (B), and (D)–(K) are representative of two independent experiments performed in the indicated cell lines. Error bars denote mean ± SD of 3 replicate assays in a representative experiment. $^{*}p < 0.05$, $^{**}p < 0.01$, $^{***}p < 0.001$, unpaired two-tailed Student's *t* test.

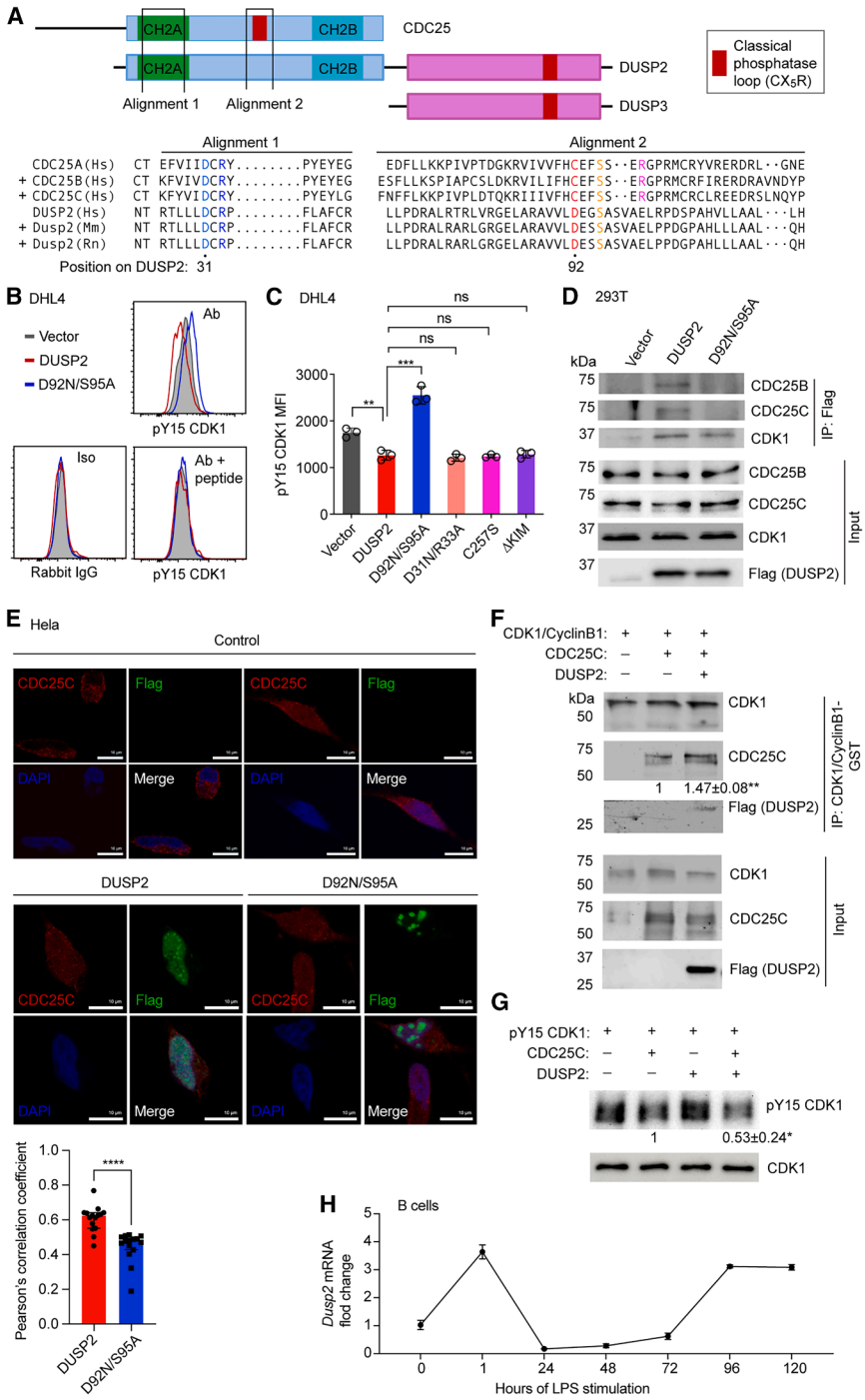

Figure 6. DUSP2 regulates CDK1 through a novel motif, which recruits CDC25s

(A) Top, domain organization of CDC25s and DUSP2. DUSP3, a member of the atypical DUSPs harboring no CDC25 homology region, was included for comparison. Bottom, alignment of CDC25s with the N-terminal region of DUSP2. The alignment was compiled on the basis of that reported by Hofmann et al.[50]; "+" marked sequences manually added on the basis on local sequence homology. Two conserved motifs and highly conserved residues within the motifs are marked by colors. Hs, human; Mm, mouse; Rn, rat.

(B) Detection of pY15-CDK1, by intracellular FACS analysis, in DHL4 cells transduced to express DUSP2, DUSP2$^{D92N/S95A}$, or vector control. After fixation and permeabilization, cells were incubated with pY15-CDK1 antibody (Ab) or rabbit IgG isotype control (Iso) or pY15-CDK1 antibody plus pY15-CDK1 blocking peptide (peptide), followed by FACS analysis.

(C) Summary and quantification of pY15-CDK1 levels measured by FACS in DHL4 cells transduced to express the indicated DUSP2 variants.

(D) 293T cells were transfected to express DUSP2, DUSP2$^{D92N/S95A}$, or vector control, and subjected to IP with anti-Flag, followed by IB with anti-CDC25B,

(legend continued on next page)

at least in part, to the constitutive BCR and/or NF-κB signaling (see results section); in adult T cell leukemia, to the HTLV-encoded transactivator Tax.[18] There is little evidence of direct genetic mechanisms causing *DUSP2* overexpression: analyses of large numbers of DLBCL biopsies and cell lines detected virtually no copy number gain at the *DUSP2* locus and only a low frequency of sporadic mutations. Recently, a high rate of DUSP2 mutation was reported in nodular lymphocyte-predominant Hodgkin lymphomas (NLPHL), yet none of the mutations targeted known functional motifs (there was also no detectable correlation between DUSP2 mutation status and phosphorylation of ERK, JNK, or p38).[55] Similarly, high rates of DUSP2 mutation were reported in several other forms of B-cell lymphoma.[56–58] Whether DUSP2 mutations in these B-cell lymphomas are functionally significant or simply indicative of a high mutation burden (potentially influencing immunogenicity) remains to be elucidated.

Our data indicate that Dusp2 expression can also enhance primary B- and T-lymphocyte proliferation (Figures 3G and 3H). However, Dusp2 expression has been shown to be transient, occurring within the first 24 h following B- and T cell activation[4,7,9] (Figure S2), while cell division usually occurs after 40 h[59] (Figure 3G). The correlation between Dusp2 expression and primary lymphocyte proliferation emerges at later time points, where *Dusp2* transcription is consistently elevated in the fast-proliferating cells (Figure 6H). This is in line with the finding of high *DUSP2* expression in GC B cells, which are in a proliferative state, compared with resting (naive) B cells (Figure 1B). Taken together, our data and the literature suggest that Dusp2 exhibits biphasic expression in antigen/mitogen-activated lymphocytes. In the early phase of activation, Dusp2 evidently dephosphorylates MAPK ERK through its phosphatase function[7,10] (Figure S5B), with an unclear effect on cellular proliferation, as the cells are still some time away from division. In the later, proliferation phase, Dusp2 serves to promote cell cycle progression by enhancing CDK1 activation through a DxxS motif unrelated to its phosphatase function that recruits CDC25s to dephosphorylate CDK1. More detailed understanding of the interaction among DUSP2, CDC25, and CDK1 will require advanced structural work[60] and additional biochemical analyses. Furthermore, it is worth noting that although the observed effects of *DUSP2*-knockdown on lymphoma cell cycle progression (Figures 5H and 5I) are consistent with the recent finding that CDK1 is not only essential for G2/M transition but also has a role in G1/S transition,[47] there is a possibility that DUSP2 also interacts with other targets to regulate the latter process.

The CDC25-CDK1 axis for cell cycle regulation functions from single-celled eukaryotic organisms all the way to mammals.[61,62] The data presented in this work indicate that DUSP2 provides a new layer of cell cycle regulation to the fundamental CDC25-CDK1 axis, in immune cells. Given that the cell cycle machinery has been mostly studied in unicellular yeasts, early embryos of frogs and fruit flies, and some mammalian cell lines,[63] but barely, if ever, in immune cells, this finding is of particular significance. It also suggests physiological importance of DUSP2 in the immune system: perhaps it endows immune cells with a superior ability for rapid expansion, which is a must for successful defense against aggressive pathogens, albeit not necessary for immune cell development.[4,8] This possibility warrants further investigation.

Overall, this work reveals an oncogenic role and its molecular mechanism for constitutive DUSP2 expression in B-cell malignancies, and suggests a similar role in other hematologic malignancies. DUSP2 lies downstream of multiple oncogenic signaling pathways to promote cell cycle progression, facilitating the transformation and maintenance of malignant cells, and thus represents an appealing therapeutic target. In this regard, the DxxS motif, discovered in the present work, provides a potential target site for developing small-molecule inhibitors that may specifically ablate DUSP2's CDK1-activating function while preserving its MAPK-suppressing activity.

Limitations of the study

Our study has several limitations that should be acknowledged and addressed in future investigations. Our attempts to validate commercially available antibodies against mouse or human DUSP2 did not identify a suitable one. As such, we were unable to assess endogenous DUSP2 protein expression in activated immune cells and various hematologic malignancies. Lacking a DUSP2-specific antibody also prevented us from investigating the regulatory mechanisms governing DUSP2 protein stability. These important questions warrant further study.

RESOURCE AVAILABILITY

Lead contact

Requests for further information and resources should be directed to and will be fulfilled by the lead contact, Baochun Zhang (baochun_zhang@dfci.harvard.edu).

Materials availability

Materials generated in this study, particularly plasmids harboring DUSP2 variants and the *Dusp2*^{stopFl} mouse line, are available upon request from

-CDC25C, and -CDK1.

(E) HeLa cells transfected with Flag-tagged WT DUSP2 or the D92N/S95A mutant were subjected to confocal imaging analysis (see STAR Methods). Scale bars, 10 μm. Pearson's correlation coefficient was calculated and shown in the graph below; each dot represents a single cell.

(F) Binding reaction mixtures of the indicated recombinant proteins were subjected to GST pull-down (IP), followed by IB with anti-CDK1, -CDC25C, and -Flag. Numbers below bands indicate quantifications (normalized to the respective CDK1 signals) relative to the indicated control reaction (shown as mean ± SD; $p = 0.001$, unpaired *t* test).

(G) *In vitro* dephosphorylation of pY15-CDK1 by recombinant CDC25C with or without DUSP2. Numbers below bands indicate quantifications relative to the indicated control reaction (shown as mean ± SD; $p = 0.03$, unpaired *t* test).

(H) Mouse splenic B cells were treated with LPS for the indicated periods of time and analyzed by RT-PCR for *Dusp2* expression.

Data in (B)–(D) are representative of two independent experiments, where WT and all variants of DUSP2 carry the FLAG tag; in (F)–(G) representative of three independent experiments; in (E) and (H) representative of two independent experiments. Error bars denote mean ± SD of 3 replicate assays in a representative experiment. ns, not significant; $^{**}p < 0.01$, $^{***}p < 0.001$, unpaired two-tailed Student's *t* test.

the lead contact with a completed materials transfer agreement and reasonable compensation by requestor for processing and shipping.

Data and code availability

- This paper analyzes existing, publicly available data, accessible through the database and links provided in the key resources table. Original western blots are available in Data S1. Microscopy data reported in this paper will be shared by the lead contact upon request.
- This paper does not report original code.
- Any additional information required to reanalyze the data reported in this paper is available from the lead contact upon request.

ACKNOWLEDGMENTS

We thank D.P. Leahy, B. Beaulieu, R. Avalos, and D. McDermott for administrative assistance; DFCI Hematologic Neoplasia Flow Cytometry Core for assistance with the flow cytometry studies and cell sorting; and K. Huang and Molecular Imaging Core for assistance with the confocal microscopy studies. We thank P. McCaffrey for valuable input. We are grateful to the NIH Tetramer Facility at Emory University for providing the PE-conjugated mCD1d-PBS57 tetramer. This work was supported by the DFCI Faculty Startup Funds and the Concern Foundation Conquer Cancer Now Award to B.Z. S.K.D. is supported by the Bill and Melinda Gates Foundation.

AUTHOR CONTRIBUTIONS

Y.Q., J.P., and B.Z. designed research; Y.Q., J.P., X. Zhang, X. Zhao, Z.W., A.Z., Q.K., J.Z., P.Y., L.Z., M.H., I.-K.C., and J.G. performed research and analyzed data; B.C. and M.A.S. contributed *DUSP2* genetic and expression data and analyses in human lymphomas; M.A.S. contributed human DLBCL cell lines; D.C. and K.R. contributed in *Dusp2* mutation analysis in mouse lymphomas; Y.Q., B.Z., and S.K.D. generated $Dusp2^{stopFl}$ mice; Y.Q., X. Zhao, and Z.W. identified and characterized the $DxxS_{92\text{-}95}$ motif; P.Z. and H.W. expressed and purified DUSP2 variants from bacteria for *in vitro* phosphatase assays; S.R. and O.P. performed histological analysis; S.A.G. provided guidance on cell cycle related assays; T.P. and S.J. performed *in vitro* protein binding study; Y.Q., J.P., and B.Z. interpreted the results and wrote the paper; B.Z. supervised the research.

DECLARATION OF INTERESTS

The authors declare no potential conflicts of interest.

STAR★METHODS

Detailed methods are provided in the online version of this paper and include the following:

SUPPLEMENTAL INFORMATION

Supplemental information can be found online at https://doi.org/10.1016/j.celrep.2026.117652.

Received: December 18, 2025
Revised: May 19, 2026
Accepted: June 17, 2026

REFERENCES

1. Jeffrey, K.L., Camps, M., Rommel, C., and Mackay, C.R. (2007). Targeting dual-specificity phosphatases: manipulating MAP kinase signalling and immune responses. Nat. Rev. Drug Discov. *6*, 391–403.
2. Fauman, E.B., Cogswell, J.P., Lovejoy, B., Rocque, W.J., Holmes, W., Montana, V.G., Piwnica-Worms, H., Rink, M.J., and Saper, M.A. (1998). Crystal structure of the catalytic domain of the human cell cycle control phosphatase, Cdc25A. Cell *93*, 617–625.
3. Huang, C.Y., and Tan, T.H. (2012). DUSPs, to MAP kinases and beyond. Cell Biosci. *2*, 24.
4. Lu, D., Liu, L., Ji, X., Gao, Y., Chen, X., Liu, Y., Liu, Y., Zhao, X., Li, Y., Li, Y., et al. (2015). The phosphatase DUSP2 controls the activity of the transcription activator STAT3 and regulates TH17 differentiation. Nat. Immunol. *16*, 1263–1273.
5. Kinney, C.M., Chandrasekharan, U.M., Yang, L., Shen, J., Kinter, M., McDermott, M.S., and DiCorleto, P.E. (2009). Histone H3 as a novel substrate for MAP kinase phosphatase-1. Am. J. Physiol. Cell Physiol. *296*, C242–C249.
6. Li, J.P., Yang, C.Y., Chuang, H.C., Lan, J.L., Chen, D.Y., Chen, Y.M., Wang, X., Chen, A.J., Belmont, J.W., and Tan, T.H. (2014). The phosphatase JKAP/DUSP22 inhibits T-cell receptor signalling and autoimmunity by inactivating Lck. Nat. Commun. *5*, 3618.
7. Rohan, P.J., Davis, P., Moskaluk, C.A., Kearns, M., Krutzsch, H., Siebenlist, U., and Kelly, K. (1993). PAC-1: a mitogen-induced nuclear protein tyrosine phosphatase. Science *259*, 1763–1766.
8. Jeffrey, K.L., Brummer, T., Rolph, M.S., Liu, S.M., Callejas, N.A., Grumont, R.J., Gillieron, C., Mackay, F., Grey, S., Camps, M., et al. (2006). Positive regulation of immune cell function and inflammatory responses by phosphatase PAC-1. Nat. Immunol. *7*, 274–283.
9. Grumont, R.J., Rasko, J.E., Strasser, A., and Gerondakis, S. (1996). Activation of the mitogen-activated protein kinase pathway induces transcription of the PAC-1 phosphatase gene. Mol. Cell Biol. *16*, 2913–2921.
10. Ward, Y., Gupta, S., Jensen, P., Wartmann, M., Davis, R.J., and Kelly, K. (1994). Control of MAP kinase activation by the mitogen-induced threonine/tyrosine phosphatase PAC1. Nature *367*, 651–654.
11. Kelly, K., and Siebenlist, U. (1995). Immediate-early genes induced by antigen receptor stimulation. Curr. Opin. Immunol. *7*, 327–332.
12. Shen, Y.H., Godlewski, J., Zhu, J., Sathyanarayana, P., Leaner, V., Birrer, M.J., Rana, A., and Tzivion, G. (2003). Cross-talk between JNK/SAPK and ERK/MAPK pathways: sustained activation of JNK blocks ERK activation by mitogenic factors. J. Biol. Chem. *278*, 26715–26721.
13. Lu, D., Liu, L., Sun, Y., Song, J., Yin, Q., Zhang, G., Qi, F., Hu, Z., Yang, Z., Zhou, Z., et al. (2020). The phosphatase PAC1 acts as a T cell suppressor and attenuates host antitumor immunity. Nat. Immunol. *21*, 287–297.

14. Dhillon, A.S., Hagan, S., Rath, O., and Kolch, W. (2007). MAP kinase signalling pathways in cancer. Oncogene *26*, 3279–3290.

15. Wada, T., and Penninger, J.M. (2004). Mitogen-activated protein kinases in apoptosis regulation. Oncogene *23*, 2838–2849.

16. Yin, Y., Liu, Y.X., Jin, Y.J., Hall, E.J., and Barrett, J.C. (2003). PAC1 phosphatase is a transcription target of p53 in signalling apoptosis and growth suppression. Nature *422*, 527–531.

17. Lin, S.C., Chien, C.W., Lee, J.C., Yeh, Y.C., Hsu, K.F., Lai, Y.Y., Lin, S.C., and Tsai, S.J. (2011). Suppression of dual-specificity phosphatase-2 by hypoxia increases chemoresistance and malignancy in human cancer cells. J. Clin. Investig. *121*, 1905–1916.

18. Kelly, K., Davis, P., Mitsuya, H., Irving, S., Wright, J., Grassmann, R., Fleckenstein, B., Wano, Y., Greene, W., and Siebenlist, U. (1992). A high proportion of early response genes are constitutively activated in T cells by HTLV-I. Oncogene *7*, 1463–1470.

19. Basso, K., Margolin, A.A., Stolovitzky, G., Klein, U., Dalla-Favera, R., and Califano, A. (2005). Reverse engineering of regulatory networks in human B cells. Nat. Genet. *37*, 382–390.

20. Brune, V., Tiacci, E., Pfeil, I., Döring, C., Eckerle, S., van Noesel, C.J.M., Klapper, W., Falini, B., von Heydebreck, A., Metzler, D., et al. (2008). Origin and pathogenesis of nodular lymphocyte-predominant Hodgkin lymphoma as revealed by global gene expression analysis. J. Exp. Med. *205*, 2251–2268.

21. Haslinger, C., Schweifer, N., Stilgenbauer, S., Döhner, H., Lichter, P., Kraut, N., Stratowa, C., and Abseher, R. (2004). Microarray gene expression profiling of B-cell chronic lymphocytic leukemia subgroups defined by genomic aberrations and VH mutation status. J. Clin. Oncol. *22*, 3937–3949.

22. Alizadeh, A.A., Eisen, M.B., Davis, R.E., Ma, C., Lossos, I.S., Rosenwald, A., Boldrick, J.C., Sabet, H., Tran, T., Yu, X., et al. (2000). Distinct types of diffuse large B-cell lymphoma identified by gene expression profiling. Nature *403*, 503–511.

23. Monti, S., Savage, K.J., Kutok, J.L., Feuerhake, F., Kurtin, P., Mihm, M., Wu, B., Pasqualucci, L., Neuberg, D., Aguiar, R.C.T., et al. (2005). Molecular profiling of diffuse large B-cell lymphoma identifies robust subtypes including one characterized by host inflammatory response. Blood *105*, 1851–1861.

24. Lenz, G., Wright, G., Dave, S.S., Xiao, W., Powell, J., Zhao, H., Xu, W., Tan, B., Goldschmidt, N., Iqbal, J., et al. (2008). Stromal gene signatures in large-B-cell lymphomas. N. Engl. J. Med. *359*, 2313–2323.

25. Chapuy, B., Stewart, C., Dunford, A.J., Kim, J., Kamburov, A., Redd, R.A., Lawrence, M.S., Roemer, M.G.M., Li, A.J., Ziepert, M., et al. (2018). Molecular subtypes of diffuse large B cell lymphoma are associated with distinct pathogenic mechanisms and outcomes. Nat. Med. *24*, 679–690.

26. Lohr, J.G., Stojanov, P., Lawrence, M.S., Auclair, D., Chapuy, B., Sougnez, C., Cruz-Gordillo, P., Knoechel, B., Asmann, Y.W., Slager, S.L., et al. (2012). Discovery and prioritization of somatic mutations in diffuse large B-cell lymphoma (DLBCL) by whole-exome sequencing. Proc. Natl. Acad. Sci. USA *109*, 3879–3884.

27. Morin, R.D., Mungall, K., Pleasance, E., Mungall, A.J., Goya, R., Huff, R.D., Scott, D.W., Ding, J., Roth, A., Chiu, R., et al. (2013). Mutational and structural analysis of diffuse large B-cell lymphoma using whole-genome sequencing. Blood *122*, 1256–1265.

28. Schmitz, R., Wright, G.W., Huang, D.W., Johnson, C.A., Phelan, J.D., Wang, J.Q., Roulland, S., Kasbekar, M., Young, R.M., Shaffer, A.L., et al. (2018). Genetics and Pathogenesis of Diffuse Large B-Cell Lymphoma. N. Engl. J. Med. *378*, 1396–1407.

29. Reddy, A., Zhang, J., Davis, N.S., Moffitt, A.B., Love, C.L., Waldrop, A., Leppa, S., Pasanen, A., Meriranta, L., Karjalainen-Lindsberg, M.L., et al. (2017). Genetic and Functional Drivers of Diffuse Large B Cell Lymphoma. Cell *171*, 481–494.e15.

30. Zhang, B., Calado, D.P., Wang, Z., Fröhler, S., Köchert, K., Qian, Y., Koralov, S.B., Schmidt-Supprian, M., Sasaki, Y., Unitt, C., et al. (2015). An Oncogenic Role for Alternative NF-kappaB Signaling in DLBCL Revealed upon Deregulated BCL6 Expression. Cell Rep. *11*, 715–726.

31. Young, R.M., Shaffer, A.L., 3rd, Phelan, J.D., and Staudt, L.M. (2015). B-cell receptor signaling in diffuse large B-cell lymphoma. Semin. Hematol. *52*, 77–85.

32. Chen, L., Monti, S., Juszczynski, P., Ouyang, J., Chapuy, B., Neuberg, D., Doench, J.G., Bogusz, A.M., Habermann, T.M., Dogan, A., et al. (2013). SYK inhibition modulates distinct PI3K/AKT- dependent survival pathways and cholesterol biosynthesis in diffuse large B cell lymphomas. Cancer Cell *23*, 826–838.

33. Davis, R.E., Ngo, V.N., Lenz, G., Tolar, P., Young, R.M., Romesser, P.B., Kohlhammer, H., Lamy, L., Zhao, H., Yang, Y., et al. (2010). Chronic active B-cell-receptor signalling in diffuse large B-cell lymphoma. Nature *463*, 88–92.

34. Srinivas, S., Watanabe, T., Lin, C.S., William, C.M., Tanabe, Y., Jessell, T.M., and Costantini, F. (2001). Cre reporter strains produced by targeted insertion of EYFP and ECFP into the ROSA26 locus. BMC Dev. Biol. *1*, 4.

35. Rickert, R.C., Roes, J., and Rajewsky, K. (1997). B lymphocyte-specific, Cre-mediated mutagenesis in mice. Nucleic Acids Res. *25*, 1317–1318.

36. Casola, S., Cattoretti, G., Uyttersprot, N., Koralov, S.B., Seagal, J., Hao, Z., Waisman, A., Egert, A., Ghitza, D., and Rajewsky, K. (2006). Tracking germinal center B cells expressing germ-line immunoglobulin gamma1 transcripts by conditional gene targeting. Proc. Natl. Acad. Sci. USA *103*, 7396–7401.

37. Calado, D.P., Zhang, B., Srinivasan, L., Sasaki, Y., Seagal, J., Unitt, C., Rodig, S., Kutok, J., Tarakhovsky, A., Schmidt-Supprian, M., and Rajewsky, K. (2010). Constitutive canonical NF-kappaB activation cooperates with disruption of BLIMP1 in the pathogenesis of activated B cell-like diffuse large cell lymphoma. Cancer Cell *18*, 580–589.

38. Cattoretti, G., Pasqualucci, L., Ballon, G., Tam, W., Nandula, S.V., Shen, Q., Mo, T., Murty, V.V., and Dalla-Favera, R. (2005). Deregulated BCL6 expression recapitulates the pathogenesis of human diffuse large B cell lymphomas in mice. Cancer Cell *7*, 445–455.

39. Pasqualucci, L., Trifonov, V., Fabbri, G., Ma, J., Rossi, D., Chiarenza, A., Wells, V.A., Grunn, A., Messina, M., Elliot, O., et al. (2011). Analysis of the coding genome of diffuse large B-cell lymphoma. Nat. Genet. *43*, 830–837.

40. Chu, Y., Solski, P.A., Khosravi-Far, R., Der, C.J., and Kelly, K. (1996). The mitogen-activated protein kinase phosphatases PAC1, MKP-1, and MKP-2 have unique substrate specificities and reduced activity in vivo toward the ERK2 sevenmaker mutation. J. Biol. Chem. *271*, 6497–6501.

41. Schmid, C.A., Robinson, M.D., Scheifinger, N.A., Müller, S., Cogliatti, S., Tzankov, A., and Müller, A. (2015). DUSP4 deficiency caused by promoter hypermethylation drives JNK signaling and tumor cell survival in diffuse large B cell lymphoma. J. Exp. Med. *212*, 775–792.

42. Malumbres, M., and Barbacid, M. (2009). Cell cycle, CDKs and cancer: a changing paradigm. Nat. Rev. Cancer *9*, 153–166.

43. Hochegger, H., Takeda, S., and Hunt, T. (2008). Cyclin-dependent kinases and cell-cycle transitions: does one fit all? Nat. Rev. Mol. Cell Biol. *9*, 910–916.

44. Santamaría, D., Barrière, C., Cerqueira, A., Hunt, S., Tardy, C., Newton, K., Cáceres, J.F., Dubus, P., Malumbres, M., and Barbacid, M. (2007). Cdk1 is sufficient to drive the mammalian cell cycle. Nature *448*, 811–815.

45. Rudolph, J. (2007). Inhibiting transient protein-protein interactions: lessons from the Cdc25 protein tyrosine phosphatases. Nat. Rev. Cancer *7*, 202–211.

46. Boutros, R., Lobjois, V., and Ducommun, B. (2007). CDC25 phosphatases in cancer cells: key players? Good targets? Nat. Rev. Cancer *7*, 495–507.

47. Suski, J.M., Ratnayeke, N., Braun, M., Zhang, T., Strmiska, V., Michowski, W., Can, G., Simoneau, A., Snioch, K., Cup, M., et al. (2022). CDC7-independent G1/S transition revealed by targeted protein degradation. Nature *605*, 357–365.

48. Vitale, I., Galluzzi, L., Castedo, M., and Kroemer, G. (2011). Mitotic catastrophe: a mechanism for avoiding genomic instability. Nat. Rev. Mol. Cell Biol. *12*, 385–392.

49. Alonso, A., Sasin, J., Bottini, N., Friedberg, I., Friedberg, I., Osterman, A., Godzik, A., Hunter, T., Dixon, J., and Mustelin, T. (2004). Protein tyrosine phosphatases in the human genome. Cell *117*, 699–711.

50. Hofmann, K., Bucher, P., and Kajava, A.V. (1998). A model of Cdc25 phosphatase catalytic domain and Cdk-interaction surface based on the presence of a rhodanese homology domain. J. Mol. Biol. *282*, 195–208.

51. Pasqualucci, L., and Dalla-Favera, R. (2015). The genetic landscape of diffuse large B-cell lymphoma. Semin. Hematol. *52*, 67–76.

52. Jiang, Y., and Melnick, A. (2015). The epigenetic basis of diffuse large B-cell lymphoma. Semin. Hematol. *52*, 86–96.

53. Shaffer, A.L., 3rd, Young, R.M., and Staudt, L.M. (2012). Pathogenesis of human B cell lymphomas. Annu. Rev. Immunol. *30*, 565–610.

54. Kristjánsdóttir, K., and Rudolph, J. (2004). Cdc25 phosphatases and cancer. Chem. Biol. *11*, 1043–1051.

55. Hartmann, S., Schuhmacher, B., Rausch, T., Fuller, L., Döring, C., Weniger, M., Lollies, A., Weiser, C., Thurner, L., Rengstl, B., et al. (2016). Highly recurrent mutations of SGK1, DUSP2 and JUNB in nodular lymphocyte predominant Hodgkin lymphoma. Leukemia *30*, 844–853.

56. Schuhmacher, B., Bein, J., Rausch, T., Benes, V., Tousseyn, T., Vornanen, M., Ponzoni, M., Thurner, L., Gascoyne, R., Steidl, C., et al. (2019). JUNB, DUSP2, SGK1, SOCS1 and CREBBP are frequently mutated in T-cell/histiocyte-rich large B-cell lymphoma. Haematologica *104*, 330–337.

57. Zhu, Q., Wang, J., Zhang, W., Zhu, W., Wu, Z., Chen, Y., Chen, M., Zheng, L., Tang, J., Zhang, S., et al. (2022). Whole-Genome/Exome Sequencing Uncovers Mutations and Copy Number Variations in Primary Diffuse Large B-Cell Lymphoma of the Central Nervous System. Front. Genet. *13*, 878618.

58. Noerenberg, D., Briest, F., Hennch, C., Yoshida, K., Hablesreiter, R., Takeuchi, Y., Ueno, H., Staiger, A.M., Ziepert, M., Asmar, F., et al. (2024). Genetic Characterization of Primary Mediastinal B-Cell Lymphoma: Pathogenesis and Patient Outcomes. J. Clin. Oncol. *42*, 452–466.

59. Dowling, M.R., Kan, A., Heinzel, S., Zhou, J.H.S., Marchingo, J.M., Wellard, C.J., Markham, J.F., and Hodgkin, P.D. (2014). Stretched cell cycle model for proliferating lymphocytes. Proc. Natl. Acad. Sci. USA *111*, 6377–6382.

60. Rowland, R.J., Korolchuk, S., Salamina, M., Tatum, N.J., Ault, J.R., Hart, S., Turkenburg, J.P., Blaza, J.N., Noble, M.E.M., and Endicott, J.A. (2024). Cryo-EM structure of the CDK2-cyclin A-CDC25A complex. Nat. Commun. *15*, 6807.

61. Malumbres, M. (2014). Cyclin-dependent kinases. Genome Biol. *15*, 122.

62. Russell, P., and Nurse, P. (1986). cdc25+ functions as an inducer in the mitotic control of fission yeast. Cell *45*, 145–153.

63. Tang, Z. (2016). Model Organisms for Studying the Cell Cycle. Methods Mol. Biol. *1342*, 21–57.

64. Xiao, C., Srinivasan, L., Calado, D.P., Patterson, H.C., Zhang, B., Wang, J., Henderson, J.M., Kutok, J.L., and Rajewsky, K. (2008). Lymphoproliferative disease and autoimmunity in mice with increased miR-17-92 expression in lymphocytes. Nat. Immunol. *9*, 405–414.

65. Barretina, J., Caponigro, G., Stransky, N., Venkatesan, K., Margolin, A.A., Kim, S., Wilson, C.J., Lehár, J., Kryukov, G.V., Sonkin, D., et al. (2012). The Cancer Cell Line Encyclopedia enables predictive modelling of anticancer drug sensitivity. Nature *483*, 603–607.

66. Koralov, S.B., Muljo, S.A., Galler, G.R., Krek, A., Chakraborty, T., Kanellopoulou, C., Jensen, K., Cobb, B.S., Merkenschlager, M., Rajewsky, N., and Rajewsky, K. (2008). Dicer ablation affects antibody diversity and cell survival in the B lymphocyte lineage. Cell *132*, 860–874.

67. Delbos, F., De Smet, A., Faili, A., Aoufouchi, S., Weill, J.C., and Reynaud, C.A. (2005). Contribution of DNA polymerase eta to immunoglobulin gene hypermutation in the mouse. J. Exp. Med. *201*, 1191–1196.

68. Kim, S.Y., and Hakoshima, T. (2019). GST Pull-Down Assay to Measure Complex Formations. Methods Mol. Biol. *1893*, 273–280.

69. Bolte, S., and Cordelières, F.P. (2006). A guided tour into subcellular colocalization analysis in light microscopy. J. Microsc. *224*, 213–232.

70. Dunn, K.W., Kamocka, M.M., and McDonald, J.H. (2011). A practical guide to evaluating colocalization in biological microscopy. Am. J. Physiol. Cell Physiol. *300*, C723–C742.

71. Li, G., Elder, R.T., Qin, K., Park, H.U., Liang, D., and Zhao, R.Y. (2007). Phosphatase type 2A-dependent and -independent pathways for ATR phosphorylation of Chk1. J. Biol. Chem. *282*, 7287–7298.

STAR★METHODS

KEY RESOURCES TABLE

REAGENT or RESOURCE	SOURCE	IDENTIFIER
Antibodies		
Anti-Flag (clone M2)	Sigma-Aldrich	Cat#F1804
Anti mouse CD19-PB (clone 6D5)	Biolegend	Cat#115526
Anti mouse CD4-AF700 (clone GK1.5)	Biolegend	Cat#100430
Anti mouse CD8-PE (clone 53-6.7)	Biolegend	Cat#100707
Anti mouse CD25-PerCP (clone PC61)	Biolegend	Cat#102027
Anti mouse CD38-APC (clone 90)	Biolegend	Cat# 102711
Anti Fas PE-Cy-7 (clone Jo2)	BD Pharmingen	Cat#557653; RRID:AB_396768
Anti-IgM	Jackson ImmunoResearch	Cat#115-006-020; RRID: AB_2338469
Anti-CD40 (clone HM40-3)	Biolegend	Cat#102902
Anti-B220	Abcam	Cat#ab550286
Anti-GFP	Abcam	Cat#ab6556
Anti-CDK1 (clone 17)	Santa Cruz	Cat# SC-54
Anti-pY15-CDK1	Cell Signaling Technology	Cat#9111T
Anti- pT14-CDK1	Cell Signaling Technology	Cat#2543
Anti-*p*-ERK	Cell Signaling Technology	Cat#4370
Anti-*p*-JNK	Cell Signaling Technology	Cat#9251
Anti-p-p38	Cell Signaling Technology	Cat#9216
Anti-ERK	Cell Signaling Technology	Cat#9102
Anti-JNK	Cell Signaling Technology	Cat#9252
Anti-p38	Cell Signaling Technology	Cat#9212
Anti-phospho-Histone H3 Ser10	Cell Signaling Technology	Cat#9701
Anti-CDC25C	Cell Signaling Technology	Cat#4688
Bacterial and virus strains		
MSCV encoding WT *Dusp2*, various *Dusp2* mutants or the vector control	This paper	N/A
Chemicals, peptides, and recombinant proteins		
Recombinant IL-4	R&D systems	Cat#404-ML
CDK1 Antibody (Y15) Blocking Peptide	Abgent	Cat#BP7517e
Lipopolysaccharides from *Escherichia coli* 055:B5	Sigma-Aldrich	Cat#L2880-100MG
CellTrace™ violet	Invitrogen	Cat# C34557
LY294002 (PI3-K Inhibitor)	ECHELON BIOSCIENCES	Cat#B-0294-5
R406	Laboratory of Margaret Shipp	N/A
GST-tagged CDK1/CyclinB1	Sigma-Aldrich	Cat#SRP5009
CDC25C	Euprotein	Cat#EP8545981
Critical commercial assays		
Annexin-V/PI staining Kit	BD Biosciences	Cat#560931
Active Caspase-3 Apoptosis Kit;	BD Biosciences	Cat#571606
QuikChange site-directed mutagenesis	Stratagene	Cat#200523
ThermoScript RT-PCR System	Invitrogen	Cat#11146-024
SYBR™ Green Universal Master Mix	Applied Biosystems	Cat#4309155
SilverQuest™ Silver Staining Kit	Thermofisher	Cat#LC6070
FITC BrdU Flow Kit	BD Biosciences	Cat#559619

(*Continued on next page*)

Continued

REAGENT or RESOURCE	SOURCE	IDENTIFIER
Hoechst 33342 solution	Thermo Fisher Scientific	Cat#62249
Deposited data		
Gene expression in primary human lymphomas	Brune et al.[20]	GEO: GSE12453
Gene expression profiling of DLBCL patient samples	Lenz et al.[24]	GEO: GSE10846
Gene expression profiles of human DLBCLs	Chapuy et al.[25]	GEO: GSE98588
Gene expression of human DLBCLs	DepMap Portal	https://depmap.org/portal/
Gene expression in human cancer cell lines	CCLE	https://portals.broadinstitute.org/ccle
Experimental models: Cell lines		
DHL4	Laboratory of Margaret Shipp	N/A
HBL-1	Laboratory of Margaret Shipp	N/A
TMD8	Laboratory of Margaret Shipp	N/A
775	Zhang et al.[30]	N/A
293T	ATCC	CRL-3216
HeLa	ATCC	CCL-2
Experimental models: Organisms/strains		
Mouse: Rag2$^{-/-}$common γ chain$^{-/-}$ (*Rag2*$^{-/-}\gamma c^{-/-}$)	Taconic	4111
Mouse: C57BL/6	Jackson Laboratory	JAX 000664
Mouse: *CD19-cre*	Jackson Laboratory	JAX 006785
Mouse: *Cγ1-cre*	Jackson Laboratory	JAX 010611
Mouse: *YFP*^{stopFl}	Jackson Laboratory	JAX 006148
Mouse: *IμBcl6*	Laboratory of Riccardo Dalla-Favera[38]	N/A
Mouse: *Dusp2*^{stopFl}	This paper	N/A
Oligonucleotides		
DUSP2-specific shRNA 1	Sigma-Aldrich	TRCN0000235434
DUSP2-specific shRNA 2	Sigma-Aldrich	TRCN0000355665
DUSP2-specific shRNA 3	Sigma-Aldrich	TRCN0000235435
DUSP2-specific shRNA 4	Sigma-Aldrich	TRCN0000235436
See Table S4 for sequences of primers used in this work	This paper	N/A
Recombinant DNA		
Plasmid: pX330-T2A-BFP	Laboratory of Klaus Rajewsky	N/A
Plasmid: pX330-sgDusp2-T2A-BFP encoding Cas9	This paper	N/A
Plasmid: pmaxGFP	Lonza	N/A
Plasmid: pLVX-IRES-ZsGreen1	Takara Bio	Cat#632187
Software and algorithms		
GraphPad Prism (v 9.1.2)	GraphPad Software	https://www.graphpad.com
Flowjo software (v 10)	Tree Star	https://www.flowjo.com
ZEISS Arivis Pro	Carl Zeiss Microscopy GmbH	https://www.zeiss.com/microscopy/en/products/software/arivis-pro.html#LanguageSwitchOverlayCloseButton
Other		
CD1d tetramer	NIH Tetramer Facility	N/A
Puromycin	Sigma-Aldrich	P8833-10MG

EXPERIMENTAL MODEL AND STUDY PARTICIPANT DETAILS

Mouse models

To generate conditional Dusp2 transgenic mice, the Dusp2 coding sequence, preceded by the CAG promoter and a *lox*P-flanked Neo^r-STOP cassette, followed by IRES-eGFP sequences, was cloned into the Rosa26 locus.[64] Transgenic mice (*Dusp2*^{stopFl}) were generated from C57BL/6 ES cells. *CD19-cre*, *Cγ1-cre*, *IμBcl6*, and *YFP*^{stopFl} alleles (all on the C57BL/6 background) have been described.[34–36,38] *Rag2*$^{-/-}$*common γ chain*$^{-/-}$ (*Rag2*$^{-/-}$*γc*$^{-/-}$) mice were bred in our mouse colony or purchased from Taconic. Mouse cohorts for tumor development were immunized intravenously with 1x10^9 SRBCs (Cedarlane) in PBS for two times, starting at 8–10 weeks old, one month apart, and then monitored twice a week for tumor development and euthanized if signs of tumor development occurred. All animals were bred and maintained in the animal facilities at the Dana-Farber Cancer Institute (DFCI), under specific pathogen-free conditions. Both male and female mice were used in all experiments; however, they were not analyzed separately, and the study was not designed to assess the influence of sex on the experimental outcomes. All animal care and procedures followed NIH guidelines and were approved by the DFCI Institutional Animal Care and Use Committee.

Cell culture

The human DLBCL cell lines used in this work have been described previously.[32] The cell lines DHL4 and TMD8 were cultured in RPMI 1640 medium (Gibco) supplemented with 10% fetal calf serum and 2 mM glutamine; HBL-1 cells were cultured in RPMI 1640 medium supplemented with 10% fatal calf serum, 2 mM glutamine and 1% sodium pyruvate. The mouse DLBCL cell line 775, derived from a *Cγ1-cre;IμBcl6* mouse in our previous work,[30] and primary mouse B and T cells were cultured in DMEM medium (Gibco) supplemented with 10% fetal calf serum, 1X non-essential amino acids, 10 mM HEPES and 50 μM β-mercaptoethanol. The 293T and HeLa cells were cultured in DMEM supplemented with 10% fatal calf serum, 10 mM HEPES, 1 mM sodium pyruvate, and 1X non-essential amino acids. All cells were maintained at 37°C in 5% CO_2. All cell lines tested negative for mycoplasma.

METHOD DETAILS

Expression analyses of *DUSP2* in human tumors

DUSP2 transcript abundance was assessed in the following DLBCL datasets obtained either from GEO (GSE12453[20]; GSE10846[24]; GSE98588[25]) or from the DepMap Portal (https://depmap.org/portal/). Multiple probe sets per gene were collapsed by its median. *DUSP2* expression was visualized with Graph Pad Prism V7.0c for Mac as boxplot (Tukey). Differences between groups were assessed with the two-sided Mann-Whitney-U-test. mRNA expression (Affy) of *DUSP2* was also assessed in a wide array of human cancer cell lines through the Cancer Cell Line Encyclopedia (https://portals.broadinstitute.org/ccle)[65] and visualized with Graph Pad Prism V7.0c for Mac.

Flow cytometry and cell sorting

Lymphoid single-cell suspensions were stained with the following monoclonal antibodies specific for mouse CD19 (6D5), CD4 (GK1.5), CD8 (53-6.7), CD25 (PC61), CD38 (90), Fas (Jo2) from BD Biosciences, Biolegend or eBioscience, and for pY15 CDK1 (10A11) from CST. Topro3 (Invitrogen) staining was used to exclude dead cells. Intracellular staining for pY15 CDK1 was done with the Foxp3 staining buffer set (eBioscience), with or without pre-incubation with blocking peptide (BP7517e, Abgent). All samples were acquired on a FACSCanto II or LSRFortessa (BD Biosciences) and analyzed by Flowjo software (Tree Star). For CD4 T cell sorting experiments, the CD1d tetramer (NIH Tetramer Facility) was employed to exclude natural killer T cells. FACS sorting was performed using a FACSAria II (BD Biosciences).

Proliferation and apoptosis assays

Mouse splenic B cells were purified by CD43-depletion using magnetic-activated cell sorting (Miltenyi), and then cultured in the presence of 20 μg/mL LPS (Sigma), 10 μg/mL anti-IgM (Jackson ImmunoResearch), or 1 μg/mL anti-CD40 (HM40-3; eBioscience) plus 25 ng/mL IL-4 (R&D systems). Mouse splenic CD4$^+$ T cells were purified by FACS sorting, treated with TAT-Cre as previously described,[66] followed by stimulation with plate-bound anti-CD3 (145-2C11, 10 μg/mL) and anti-CD28 (37.51, 2 μg/mL) (eBioscience). To monitor cell division, the mouse splenic B and T cells, mouse lymphoma cell line 775, and human DLBCL lines (HBL1, TMD8 and DHL4) were labeled with CellTrace violet (Invitrogen), per the manufacturer's instructions. Cells undergoing apoptosis were detected by Annexin-V/PI staining (BD Biosciences) or active Caspase-3 staining (using the Active Caspase-3 Apoptosis Kit; BD Biosciences). All samples were analyzed by Flow Cytometry.

CRISPR-Cas9 editing of *Dusp2* locus in tumor cells

Mouse lymphoma cells (cell line 775) were electroporated with pX330-sgDusp2-T2A-BFP encoding Cas9 and a single-guide RNA targeting the mouse *Dusp2* coding region (the sg1-mDusp2 sequence is provided in Table S4), together with a reporter plasmid pmaxGFP. 36 h later, GFP$^+$ cells were purified by FACS sorting; an aliquot of cells was frozen down (pre-transfer cells) and the rest were transplanted into *Rag2*$^{-/-}$*γc*$^{-/-}$ mice (1 x 10^6 cells/recipient). At 4–5 weeks post-transfer, the tumor cells (CD19$^+$) were

harvested from recipients. Pre- and post-transfer cells were subjected to Sanger sequencing analysis for the targeted *Dusp2* region (primer sequences for cloning this region are provided in Table S4).

RNA interference

Human DLBCL cells (DHL4, HBL1 and TMD8) were seeded at a density of 2 x 10^5 cells/well in medium containing polybrene (at a final concentration of 8 μg/mL) in 24-well tissue culture plates (500 μL/well), inoculated with 500 μL/well of lentivirus supernatant containing either the negative control vector pLKO.1 or vectors carrying *DUSP2*-specific shRNAs (sh1, TRCN0000235434; sh2, TRCN0000355665; sh3, TRCN0000235435; sh4, TRCN0000235436; all from Sigma), and centrifuged at 460 g for 90 min. After overnight incubation, the cells were cultured in 1 mL of fresh media containing puromycin (2 μg/mL for DHL4 and HBL1; 1 μg/mL for TMD8 cells) for 2 days of selection. Knockdown efficiency was determined by real-time PCR (primer sequences are provided in Table S4).

Ectopic expression

Mouse lymphoma cells (cell line 775) were transduced with MSCV encoding WT *Dusp2*, various *Dusp2* mutants or the vector control (all carry an IRES-GFP reporter). The transduced cells (GFP^+) were either subjected to *in vitro* analyses or transplanted into $Rag2^{-/-}\gamma c^{-/-}$ mice (1 x 10^5 cells/recipient) to assess their *in vivo* growth. Human DLBCL cells were transduced with pLVX-IRES-ZsGreen1 encoding WT *DUSP2* (with or without a C-terminal FLAG tag), various *DUSP2* variants (with a C-terminal FLAG tag) or the vector control (all carry an IRES-GFP reporter), and subjected to *in vitro* analyses. *DUSP2* variants were cloned by QuikChange site-directed mutagenesis (Stratagene).

Histology and immunohistochemistry

For histological examination, tissues were fixed with 10% formalin (Sigma), and 5 μm paraffin-embedded sections were stained with hematoxylin and eosin (H&E). Immunohistochemical staining was performed on the Leica Bond automated staining platform with anti-B220 (#ab550286, Abcam) and anti-GFP (#ab6556, Abcam) antibodies using the Leica Biosystems Refine Detection Kit with citrate antigen retrieval.

Analysis of tumor clonality

Genomic DNA was isolated from tumor tissues or WT splenic B cells (as control). *IgH-V* gene rearrangements were amplified by PCR with a single reverse primer binding to a sequence within the J_H4 intronic region and a set of forward primers to detect most V_H gene families (V1-FR3, V5-FR3, V3-FR3, V7-FR3, and V9-FR3 in a 6:3:1:1:1 ratio)[67] (primer sequences are provided in Table S4).

IgH somatic mutation analysis

IgH somatic mutation analysis was performed as described previously.[30]

Quantitative RT-PCR

Total RNA was extracted using TRIzol reagent, and cDNA was synthesized using the ThermoScript RT-PCR System (Invitrogen) per the manufacturer's instructions. For real-time PCR we used Power SYBR Green, followed by analysis with the StepOnePlus system (Applied Biosystems). Samples were assayed in triplicate, and values normalized to those of *hGAPDH* (in the human), *mHPRT* or *mGAPDH* (in the mouse) (primer sequences are provided in Table S4).

Mass spectrometry

Human DLBCL cells (cell line HBL1) transduced with DUSP2-Flag, DUSP2 or vector control were lysed in lysis buffer (150 mM NaCl, 0.5% NP-40, 10% glycerol, 1 mM PMSF and a 'cocktail' of protease inhibitors). 10 mg of proteins of each lysate were immunoprecipitated with 20 μg of anti-Flag antibody (F1804, Sigma); immunoprecipitates were run on an SDS-PAGE gel, followed by staining with Pierce Silver Stain for Mass Spectrometry (#24600), per the manufacturer's instructions. Excised gel segments were submitted for mass spectrometry analysis at the Taplin Mass Spectrometry Facility at Harvard Medical School.

Co-immunoprecipitation

293T cells transfected with pLVX-IRES-ZsGreen1 encoding various *DUSP2* variants or the vector control were lysed in lysis buffer (150 mM NaCl, 0.5% NP-40, 10% glycerol, 1 mM PMSF and a "cocktail" of protease inhibitors). The lysates were immunoprecipitated with anti-CDK1 (SC-54, Santa Cruz), anti-Flag (F1804, Sigma) or control IgG. The immunoprecipitates were washed six times with the lysis buffer and subjected to SDS-PAGE, followed by immunoblot analysis.

Immunoblot analysis

Protein extracts were fractionated on 10% or 15% SDS-PAGE, transferred onto PVDF membranes, and immunoblotted with the following primary antibodies specific for Flag (F1804, Sigma), CDK1 (SC-54, Santa Cruz), pY15-CDK1 (#9111, CST), pT14-CDK1 (#2543, CST), *p*-ERK (#4370, CST), *p*-JNK (#9251, CST), p-p38 (#9216, CST), ERK (#9102, CST), JNK (#9252, CST), p38 (#9212, CST).

Cell cycle analysis

In one set of experiments, 48 h after transduction with shRNAs targeting *DUSP2*, human DLBCL cells were labeled with bromodeoxyuridine (BrdU) for 30 min before harvesting; BrdU incorporation and DNA content were analyzed with the FITC BrdU Flow Kit (BD Biosciences) per the manufacturer's instructions. In another set of experiments, 48 h after transduction with lentiviral vector encoding *DUSP2* or vector control, human DLBCL cells were stained with the Hoechst 33342 solution (Thermo Fisher Scientific) per the manufacturer's instructions. All samples were analyzed by Flow Cytometry.

Cell mitosis analysis

DHL4 cells were harvested, fixed with 4% formaldehyde, and then permeabilized in 90% methanol. After washing, the cells were stained with an antibody (#9701, CST) specific to phospho-Histone H3 Ser10 (a specific marker for mitotic cells) per the manufacturer's instructions, and analyzed by Flow Cytometry.

Chemical nhibition with LY294002 or R406

LY294002 (10 μM) or R406 (1 μM) was added to cell culture medium and cells were maintained in a 37°C incubator for 48 h, as described previously.[32] Cellular apoptosis was detected using the Active Caspase-3 Apoptosis Kit (BD Biosciences) per the manufacturer's instructions.

In vitro phosphatase assay

cDNA sequences encoding the human DUSP2 N-terminal half (aa 2–157), the 'full-length protein' (aa 2–314) with a C257S mutation, or the C-terminal half (aa 158–314), followed by a Flag-coding sequence, were subcloned into the pGEX-6P-1 expression vector (GE Healthcare), which produced the recombinant proteins with a GST tag at the N terminus. The proteins were expressed in BL21-CodonPlus (DE3)-RIPL cells (Agilent), purified by Glutathione Sepharose 4B (GE Healthcare) followed by Superdex 200 gel filtration chromatography (GE Healthcare), and then cleaved of the GST tag with PreScission Protease 3C. The cleaved C-terminal half construct (aa 158–314) was further purified by Q ion exchange column (GE Healthcare) while the other cleaved proteins were purified by Heparin affinity chromatography (GE Healthcare); all final products were in 20 mM Tris-HCl pH7.5, 150 mM NaCl, 1 mM DTT. For phosphatase assay, the reaction mixture containing 1 μg purified DUSP2 variant in 200 μL buffer (50 mM Tris-HCl pH6.8, 50 mM NaCl, 1 mM DTT, 10 mM $MgCl_2$ or $CaCl_2$) with 20 mM *p*-nitrophenylphosphate (pNPP) substrate was incubated for 60 min at 37°C. The reaction was terminated by adding 800 μL of 0.2 M NaOH and 50 mM EDTA, and the *p*-nitrophenol production was determined by measuring A410.

In vitro protein binding assay

This assay was performed as previously described[68] with modifications. Briefly, recombinant GST-tagged CDK1/CyclinB1 (SRP5009, Sigma), CDC25C (EP8545981, Euprotein), and the full-length DUSP2 with C257S mutation (as described above; the C257S mutation is irrelevant in DUSP2 regulation of CDK1) were mixed at a molar ratio of 1:2:2 and incubated in Kinase Buffer (10 mM MgCl, 10 mM NaF, 1 mM DTT, 400 μM ATP) for 1 h. Then, the reaction mixtures were added to GST resin and incubated for 30 min. The bound proteins were eluted and analyzed by SDS-PAGE with anit-CDK1 (SC-54, Santa Cruz), anti-CDC25C (#4688, CST), and anti-Flag (F1804, Sigma).

Immunofluorescence staining and confocal microscopy

HeLa cells grown on glass coverslips were transfected with plasmids encoding Flag-tagged WT DUSP2 or the D92N/S95A mutant. At 24 h after transfection, cells were washed and fixed with 4% paraformaldehyde for 10 min at room temperature, permeabilized with 0.2% Triton X-100 in 10% FBS-containing PBS for 10 min, and blocked with 10% FBS in PBS for 60 min. Cells were stained with Alexa Fluor 488-conjugated anti-DYKDDDDK Tag (Flag; clone L5; Biolegend Cat# 637317) and PE-conjugated anti-CDC25C (clone H-6; Santa Cruz Cat# sc-13138) antibodies for overnight at 4°C. Next, the cells were washed by 10% FBS-containing PBS. Coverslips were mounted using ProLong Gold Antifade Mountant with DAPI (Thermo Fisher Scientific #P36966). Confocal images were acquired by Zeiss under identical microscope settings across all samples. Of note, in some cells CDC25C exhibited mainly cytoplasmic staining while in other cells both cytoplasmic and nuclear staining as shown in control HeLa cells. Because DUSP2 is primarily a nuclear protein, the colocalization analysis in HeLa cells transfected with Flag-tagged WT DUSP2 or the D92N/S95A mutant was restricted to Flag-positive cells with nuclear CDC25C staining. Colocalization and Pearson's correlation coefficient were analyzed using ZEISS Arivis Pro and ImageJ software.[69,70]

pY15 CDK1 immunoprecipitation and *in vitro* phosphatase assay

6×10^6 DHL4 cells were treated with 1.5 mM hydroxyurea[71] for 24 h. Cells were harvested and lysed in lysis buffer supplemented with PMSF, and pY15 CDK1 was immunoprecipitated using anti-CDK1 antibody (sc-54 clone #17) overnight at 4°C. Immune complexes were captured using Dynabeads Protein G (ThermoFisher Scientific #10003D) and washed with phosphatase buffer. The beads were divided into equal aliquots, and incubated with recombinant human CDC25C (SinoBiological #C04-20CG) and/or the full-length DUSP2 (with the C257S mutation which is irrelevant in DUSP2 regulation of CDK1) at 30°C for 45 min in phosphatase buffer (25 mM Tris-HCl pH 7.4, 100 mM NaCl, 1 mM DTT, and 1 mM EDTA, without phosphatase inhibitors). Reactions were terminated

by addition of 2X SDS sample buffer and boiling. Samples were analyzed by Immunoblot with antibodies against pY15-CDK1 and total CDK1.

QUANTIFICATION AND STATISTICAL ANALYSIS

GraphPad Prism 9 software was used for statistical analysis, data visualization, and data processing. Unless otherwise indicated, data were analyzed using unpaired two-tailed Student's *t* test; a value of $p < 0.05$ was considered significant ($^{*}p < 0.05$, $^{**}p < 0.01$, $^{***}p < 0.001$, and $^{****}p < 0.0001$; ns, not significant). Survival curves were compared using the log rank test.